Accepted Manuscript

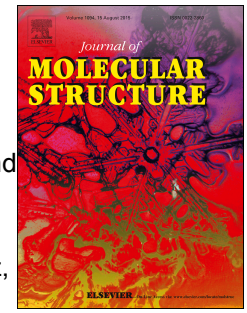

Synthesis and characterization of a series of isoniazid hydrazones. Spectroscopic and theoretical study

Verónica Ferraresi-Curotto, Gustavo A. Echeverría, Oscar E. Piro, Reinaldo Pis-Diez, Ana C. González-Baró

PII: S0022-2860(16)31308-4

DOI: 10.1016/j.molstruc.2016.12.018

Reference: MOLSTR 23216

To appear in: *Journal of Molecular Structure*

Received Date: 21 June 2016

Revised Date: 17 November 2016

Accepted Date: 5 December 2016

Please cite this article as: V. Ferraresi-Curotto, G.A. Echeverría, O.E. Piro, R. Pis-Diez, A.C. González-Baró, Synthesis and characterization of a series of isoniazid hydrazones. Spectroscopic and theoretical study, *Journal of Molecular Structure* (2017), doi: 10.1016/j.molstruc.2016.12.018.

Synthesis and characterization of a series of isoniazid hydrazones. Spectroscopic and theoretical study

Verónica Ferraresi-Curotto[1], Gustavo A. Echeverría[2], Oscar E. Piro[2], Reinaldo Pis-Diez[1], Ana C. González-Baró[1*]

[1]CEQUINOR (CONICET, UNLP), CC 962, B1900AVV, La Plata, Argentina.
[2]IFLP (CONICET, UNLP), CC 67, B1900AVV, La Plata, Argentina.
*Corresponding author: agb@quimica.unlp.edu.ar

Abstract

A family of hydrazones of isoniazid and a group of hydroxybenzalaldehydes (vanillin, 5-bromovanillin, 5-chlorosalicylaldehyde and 5-bromosalicylaldehyde) were obtained and fully characterized. The results, including theoretical data, are comparatively analyzed along with the already reported hydrazone of o-vanillin. The crystal structures of three compounds were determined. The hydrazones obtained from halogenated aldehydes are isomorphic and chiral to each other. Structures are further stabilized by (pyr)$NH^{+}\cdots Cl$ and $OwH\cdots Cl$ bonds. The vanillin hydrazone shows a conformer that differs from the previously reported. Neighboring molecules are linked to each other through $OH\cdots N$(pyr) bonds, giving rise to a nearly planar polymeric structure. The conformational space was searched and geometries were optimized both in the gas phase and including solvent effects by DFT. Results are extended to describe the 5-bromovanillin hydrazone. FTIR, NMR and electronic spectra were measured and assigned with the help of computational calculations.

Keywords: Crystal structures; spectroscopy; DFT calculations; Isoniazid; Schiff bases.

1. Introduction

The hydrazone functional group has been extensively studied [1 and references therein]. Hydrazones play important roles in various fields, from organic synthesis and medicinal chemistry to supramolecular chemistry, and have many applications. The straightforward synthesis, the possibility of including different substituents, and the stability towards hydrolysis of hydrazones can be cited as reasons for their attractiveness.

The chemical versatility of hydrazones can be mainly attributed to the functional diversity of the azomethine group, particularly the C=N–N moiety. The structure of a hydrazone shows (i) nucleophilic imine and amino-type (more reactive) nitrogens, (ii) an imine carbon that has both electrophilic and nucleophilic character, (iii) configurational isomerism stemming from the intrinsic nature of the C=N double bond, and (iv) in most cases an acidic N–H proton. These structural motifs give determines the physical and chemical properties of the hydrazone, playing a crucial role in its applications.

Hydrazones are usually obtained by condensation of one hydrazine or hydrazide with a ketone or aldehyde. The hydrazide here employed is Isoniazid, the hydrazide of isonicotinic acid (INH, see Figure 1). It has been recognized as an effective antituberculous agent and it is still employed in the treatment and prevention of this disease. However, actual formulations containing INH show several undesired side effects. On the other hand, it has been determined that hydrazones obtained from the condensation of isoniazid and some hydroxy-aldehydes are less toxic while preserving activity. This fact can be attributed to the inactivation of the NH_2 group of INH upon hydrazone formation [2 and references therein]. Moreover, hydrazones from INH are interesting chemical systems because they possess an additional nucleophilic cite, the pyridine nitrogen atom.

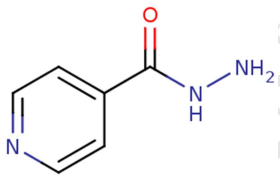

Figure 1. Structure of Isoniazid.

As part of our study on Schiff base formation with aromatic hydroxy-aldehydes [2, 3], a complete study of a family of hydrazones of INH was carried out with a group of aldehydes depicted in Figure 2, including vanillin (4-hydroxy-3-methoxybenzaldehyde, *Va*) and its derivative 3-bromo-4-hydroxy-5-methoxybenzaldehyde (5-bromovanillin, *BrVa*). Two derivatives of salicylaldehyde are also included, namely 5-chloro-2-hydroxybenzaldehyde (5-chlorosalicylaldehyde, *ClSal*) and 5-bromo-2-hydroxybenzaldehyde (5-bromosalicylaldehyde, *BrSal*).

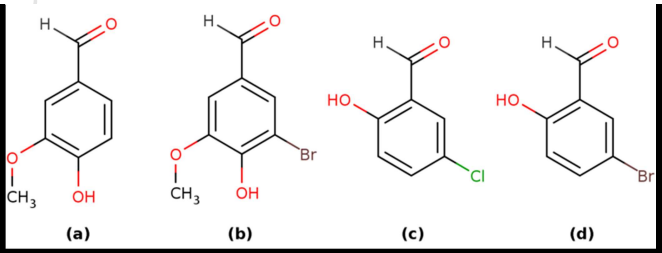

Figure 2. Structure of the hydroxyl-aldehydes. **(a)** Vanillin, **(b)** Br-vanillin, **(c)** 5-Chlorosalicylaldehyde, **(d)** 5-Bromosalicylaldehyde.

The present article involves a complete experimental and theoretical characterization of the four hydrazones and the comparative analyses with the hydrazone of *o*-vanillin (2-hydroxy-3-methoxybenzaldehyde, *o-HVa*) and INH, INHoVa, already reported by our group (Figure 3) [2].

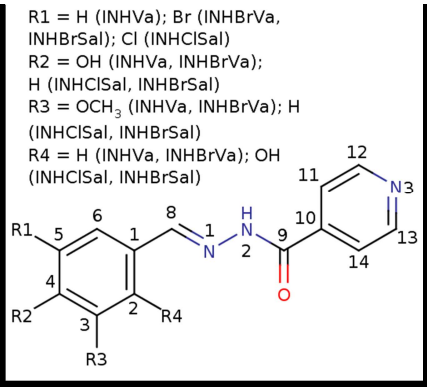

Figure 3. Structure of the obtained hydrazones.

For the compounds which afforded suitable single crystals the solid state structures were determined by X-ray diffraction methods. A detailed analysis of inter- and intra-molecular H-bonds is conducted to explain their effects on structure stabilization. FTIR, NMR and electronic absorption spectra were recorded and assigned with the assistance of results from computational methods based on the Density Functional Theory (DFT).

2. Experimental section

2.1. General procedure for the synthesis of isonicotinoyl Schiff bases

The compounds were synthesized according to an adaptation of the reported procedure for the analytical determination of Isoniazid with Va [4]. Twenty milliliters of an ethanolic solution containing 3 mmol of the aldehyde (Sigma) was drop-wise added to a solution of 1.5 mmol of Isoniazid (Sigma) in ten mL of ethanol (Merck), with continuous stirring and slight heating. Excess of aldehyde has been already employed in previous work [2] as allows obtaining the products in milder experimental conditions, avoiding reflux or long-time heating at high temperature, and have shown to improve the yield. Drops of concentrated hydrochloric acid (Merck) were added to reach a pH value of 5. Upon standing, the products were obtained and the solids were filtered out from the solution, washed repeatedly with cold ethanol and then dried in a

desiccator. Melting points were determined using a Bock monoscop "M" instrument as an additional criteria of the products.

It is worth mentioning at this point that the hydrazone obtained by the condensation reaction of INH with vanillin (INHVa) has been previously reported by other authors [5] following a different synthetic method and the crystal structure of a different conformer was already reported in the form of a monohydrate [6]. Furthermore, the compound resulting from the condensation reaction of INH with ClSal was already obtained by other authors in different conditions of synthesis [7, 8], but no crystal structure was reported.

INHVa (1): (E)-N'-(4-hydroxy-3-methoxybenzylidene)isonicotinohydrazide.

Orange solid precipitated immediately, it was further recristalized from ethanol and yellow prismatic crystals were obtained after a week (m. p. 260-263 °C).

INHBrVa (2): (E)-N'-(3-bromo-4-hydroxy-5-methoxybenzaldehyde)isonicotinohydrazide.

Orange solid not suitable for structural X-ray diffraction study precipitated after two days (m. p. 285-287 °C).

INHClSal (3): (E)-N'-(5-chloro-2-hydroxybenzaldehyde)isonicotinohydrazide.

Colorless thin prismatic crystals suitable for X-ray diffraction were obtained after eleven days (m. p. 246-248 °C).

INHBrSal (4): (E)-N'-(5-bromo-2-hydroxybenzaldehyde)isonicotinohydrazide.

Yellow crystals suitable for structural X-ray diffraction study were obtained after 24h (m. p. 259-261 °C).

2.2. X-ray diffraction data

The measurements were performed on an Oxford Xcalibur Gemini, Eos CCD diffractometer with graphite-monochromated CuKα (λ=1.54178 Å) radiation. X-ray diffraction intensities were collected (ω scans with ϑ and κ-offsets), integrated and scaled with CrysAlisPro [9] suite of programs. The unit cell parameters were obtained by least-squares refinement (based on the angular setting for all collected reflections with intensities larger than seven times the standard deviation of measurement errors) using CrysAlisPro. Data were corrected empirically for absorption employing the multi-scan method implemented in CrysAlisPro. The structures were solved by direct methods with SHELXS of the SHELX package [10] and the molecular model

developed by alternated cycles of Fourier methods and full-matrix least-squares refinement with SHELXL of the same suit of programs. The H-atoms were found at approximated positions in a difference Fourier map phased on the heavier atoms. However, all but the hydroxyl and water hydrogen atoms were located stereo-chemically and refined with the riding model. The hydroxyl and the water hydrogen atoms were refined at their found positions with isotropic displacement parameters.

The closely related chemical formula, the same space group and almost identical cell constant values strongly suggested that the bromine-containing solid was isomorphic to the chlorine-containing one. In fact, an initial molecular model assuming the same atom positions as in the chlorine crystal with the identity of the ring halogen atom changed from chlorine to bromine, lead to smooth convergence of the structural parameters for the bromide crystal during the least-squares refinement against the corresponding X-ray data set. Interestingly, the Flack's absolute structure parameter [11] (x) turned out to be x=1.01(3) thus, indicating that the bromine crystal was the chiral counterpart of the chlorine one. In fact, by inverting the molecular model, the x-value dropped to -0.03(2). The Flack's parameter is the fractional contribution to the diffraction pattern due to the molecule's racemic twin and for the correct enantiomeric crystal it should be zero to within experimental error [10].

Crystal data and structure refinement results are summarized in Table 1.

2.3. Spectroscopic analysis

The FTIR spectra were obtained with a Bruker EQUINOX 55 spectrometer in KBr discs with 4 cm^{-1} resolution and 60 scans, in the 4000-400 cm^{-1} range. ^{1}H-NMR and ^{13}C-NMR spectra were recorded as DMSO-d6 solutions, on a Bruker Advance II spectrometer at 500 MHz using tetramethylsilane as the internal reference. Electronic absorption spectra were measured on ethanolic 3 x 10^{-5} M solutions in the 200-800 nm region, with a Hewlett-Packard 8452-A diode array spectrometer using 10 mm quartz cells.

2.4. Computational methods

The conformational space of the compounds was explored with the aid of the semiempirical PM6 method [12]. Several starting geometries derived from selected variations in C14-C10-C9-N2,

C10-C9-N2-N1, N2-N1-C8-C1 and N1-C8-C1-C6 torsion angles were optimized (see Figure 3 for atom labelling). Geometries obtained from X-ray diffraction were also used as a starting point for the optimizations. The geometries were further re-optimized both in gas phase and including solvent effects using the hybrid meta-GGA M06–2X exchange–correlation density functional [13] with a triple-zeta 6–311G(d,p) basis set [14,15]. Solvent effects (ethanol) were included implicitly through the Conductor-like Polarizable Continuum Model [16,17]. Numerical integrations were carried out using a grid containing 96 radial points and 590 angular points around each atom. For compounds that involve Br atom [INHBrVA (**2**) and INHBrSal (**4**)], a grid with 160 radial points and 974 angular points was used. The critical points found after optimization were characterized by the sign of the eigenvalues of the Hessian matrix of the total electronic energy with respect to the nuclear coordinates. When the critical point corresponded to a minimum on the potential energy surface, the eigenvalues were converted to harmonic vibrational frequencies. Vibration frequencies were scaled by a factor of 0.982 to ease the comparison with experimental values [13]. Electronic transitions were calculated within the framework of the Time-Dependent DFT (TD-DFT) [18,19] using the PBE0 functional [20] and the triple zeta 6-311+G(d,p) basis set [14,15], with solvent effects, as was previously stated. Geometry optimizations, Hessian matrix calculation and diagonalization, and electronic transition calculations were performed with the GAMESS-US program [21]. Isotropic magnetic shieldings of ^{13}C and ^{1}H were calculated at the B3LYP/6–311+G(2d,p)//B3LYP/6–31G* level of theory as suggested by Cheeseman and co-workers, using the Gauge-independent Atomic Orbital method [22-24]. Isotropic magnetic shieldings were turned into chemical shifts by subtracting the corresponding isotropic magnetic shieldings of TMS, which were calculated at the same level of theory as above. Solvent effects (DMSO) were included implicitly through the Integral Equation Formalism version of the Polarizable Continuum Model [25]. Isotropic magnetic shieldings were calculated with the Gaussian 03 package [26]. The animation of the vibrational modes was done with Gabedit [27] and MO's figures were done with wxMacMolPlt [28]. Potential energy distribution analyses were carried out with the program vibca [29]. Marvin was used for drawing chemical structures [30]. Chloride counter-ion and water molecules present in the crystals were not considered in the calculations.

3. Results and Discussion

3.1. Crystallographic structural data

Crystal data and structure refinement results are summarized in Table 1 for all compounds which were suitable for crystallographic analyses.

Table 1. Crystal data and structure refinement results for (E)-N'-(5-X-2-hydroxybenzaldehyde) isonicotinohydrazide chloride hydrate (X = Cl, Br) and (E)-N-(4-hydroxy-3-methoxybenzylidene) isonicotinohydrazide hydrate.

Compound	**INHVa (1)**	**INHClSal (3)**	**INHBrSal (4)**
Empirical formula	$C_{14}H_{15}N_3O_4$	$C_{13}H_{13}Cl_2N_3O_3$	$C_{13}H_{13}BrClN_3O_3$
Formula weight (g/mol)	289.29	330.16	374.62
Temperature (K)	293(2)	295(2)	295(2)
Wavelength (Å)	1.54184	1.54184	1.54184
Crystal system	Monoclinic	Orthorhombic	Orthorhombic
Space group	$P2_1/n$	$P2_12_12_1$	$P2_12_12_1$
unit cell dimensions			
a (Å)	8.3741(6)	6.7061(2)	6.7021(1)
b (Å)	13.103(1)	13.5765(6)	13.6568(3)
c (Å)	12.683(2	15.8941(5)	15.9769(3)
β (º)	99.02(1)		
volume ($Å^3$)	1374.4(2)	1447.08(9)	1462.35(5)
Z, calc. dens. (Mg/m^3)	4, 1.398	4, 1.515	4, 1.702
Abs. Coeff. (mm^{-1})	0.874	4.171	5.648
F(000)	608	680	752
Crystal shape/color	Plate / yellow	Prism / colorless	Prism / yellow
Crystal size (mm^3)	0.269 x 0.178 x 0.015	0.793 x 0.148 x 0.074	0.581 x 0.086 x 0.066
θ-range(º) for data collection	4.88 to 70.96	4.28 to 73.31	4.26 to 71.52
Index ranges	$-10\leq h\leq 10$, $-16\leq k\leq 14$, $-15\leq l\leq 13$	$-3\leq h\leq 8$, $-15\leq k\leq 16$, $-19\leq l\leq 17$	$-8\leq h\leq 5$, $-16\leq k\leq 16$, $-19\leq l\leq 16$
Reflections collected	5778	3768	4195
Independent reflections	2638 [R(int) = 0.0417]	2610 [R(int) = 0.0216]	2426 [R(int) = 0.0161]
Observed reflections [I>2σ(I)]	1320	2329	2308

Completeness (%)	99.5 (to ϑ=70.96°)	98.4 (to ϑ=73.31°)	99.1. (to ϑ=73.31°)
Max. and min. transmission		0.7589 and 0.5735	0.6932 and 0.1472
Refinement method	Full-matrix least-squares on F^2	Full-matrix least-squares on F^2	Full-matrix least-squares on F^2
Data / restraints / parameters	2638 / 3 / 203	2610 / 0 / 202	2426 / 0 / 203
Goodness-of-fit on F^2	1.018	1.041	1.047
Final R indices[a] [I>2σ(I)]	R1 = 0.0578, wR2 = 0.1171	R1 = 0.0402, wR2 = 0.1075	R1 = 0.0289, wR2 = 0.0762
R indices (all data)	R1 = 0.1217, wR2 = 0.1597	R1 = 0.0452, wR2 = 0.1123	R1 = 0.0304, wR2 = 0.0776
Absolute structure parameter		0.00(2)	-0.03(2)
Larg. diff. peak & hole (e.Å^{-3})	0.146 and -0.191	0.217 and -0.265	0.306 and -0.272

[a] $R_1=\Sigma||F_o|-|F_c||/\Sigma|F_o|$, $wR_2=[\Sigma w(|F_o|^2-|F_c|^2)^2/\Sigma w(|F_o|^2)^2]^{1/2}$

3.1.1.(E)-N'-(4-hydroxy-3-methoxybenzylidene)isonicotinohydrazide hydrate: INHVa (1).

Figure 4 shows an ORTEP [31] drawing of the solid state structure and corresponding intra-molecular bond distances and angles are listed in the Supplementary Material, Table S1a. The organic molecule is nearly planar [*rms* deviation of non-H atoms from the best least-squares molecular plane of 0.044 Å] and closely related to the isomorphic pair (**3**) and (**4**). In fact, it can be obtained from these latter molecules by replacing the halide-substituents for a methoxy group and changing the location of the hydroxyl group from 2- to 4- position in the ring. The pyridine moiety is deprotonated, rendering the conformer electrically neutral. The main structural differences between (**1**) and the pair (**3**) and (**4**) include: (i) a shortening of the mean pyridine C-N bond length of 0.011 Å upon deprotonation and (ii) the removal of the intra-molecular OH···N bond in the isomorphic compounds and the formation of a bent OH···O(methoxy) new bond in the conformer [d(OH···O)=2.237 Å and∠ (O-H···O)=108.0º].

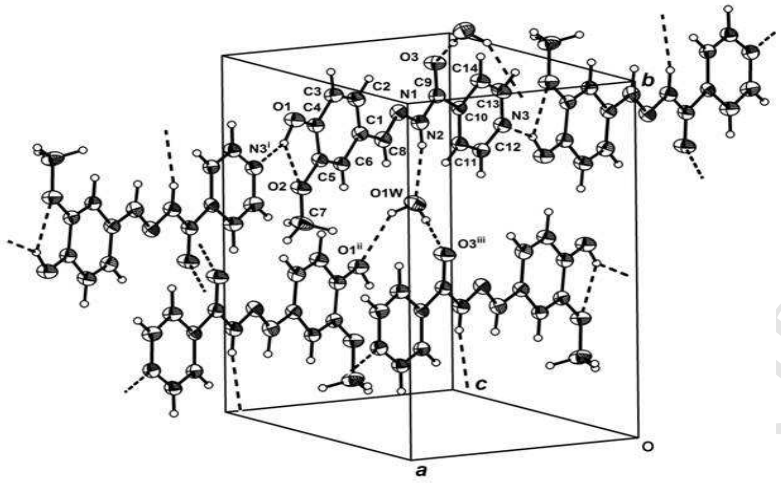

Figure 4. View of (E)-N'-(4-hydroxy-3-methoxybenzylidene)isonicotinohydrazide hydrate crystal (**1**), showing the labelling of the non-H atoms and their displacement ellipsoids at the 30% probability level. Intra- and inter-molecular H-bonds are indicated by dashed lines.

The molecular structure of a quite different conformer, also crystallized as monohydrate in the same space group $P2_1/n$, having nearly the same volume but in a different unit cell, has been reported [6]. In fact, the conformers are nearly related to each other through a rotation of about 180º around the Ph-C σ-bond (C1-C8 bond in Figure 4). Though showing a good agreement in bond distances and angles, the reported one further differs from the presented here in its appreciable deviation from planarity. As expected, the conformer crystals also differ from each other in their packing.

The mentioned differences between both conformers can be a consequence of different experimental conditions in the preparation. In the present work the crystals were obtained by letting the recrystallization solution slowly cool to room temperature and then keeping it for at least one week. The previously reported procedure describes a faster cooling followed by the separation of the product from the solution. The anhydrate of this latter conformer has been reported to crystallize in the *Cc* space group [32] and the structure of yet another closely related conformer that crystallizes in the $P2_1/c$ space group with a methanol solvent molecule has also been published [33].

Hydrogen bond distances and angles are detailed in Table S2a of the Supplementary Material. The crystal is further stabilized by inter-molecular H-bonds. Neighbouring molecules are linked

to each other through OH···Npyr bonds [d(OH···N)=1.806 Å and ∠ (O-H···N)=149.6º] giving rise to a nearly planar, ribbon-like, polymeric structure that extends along the crystal [-3, 0, 1] direction. In turn, neighbouring polymers in the lattice are bridged by the water molecule (nearly onto the molecular plane) through N-H···Ow-H1···O'carb [d(NH…Ow)=2.135 Å and ∠ (N-H···Ow)=166.7º; d(OwH1···O'carb)=1.997 Å and∠ (Ow-H1···O'carb)=168.2º] and NH.Ow-H2···O"ox [d(OwH1···O"ox)=2.247 Å and∠ (Ow-H1···O"ox)=143.3º] bonds (see Figure4).

3.1.2. (E)-N'-(5-X-2-hydroxybenzaldehyde)isonicotinhydrazide (X: Cl, Br) chloride hydrate: INHClSal (3) y INHBrSal (4).

As detailed in the experimental section, the solid state compounds are isomorphic and chiral counterparts of each other, differing only in the interchange of chlorine and bromine atoms in the aldehyde ring. In fact, the *rms* separation between homologous non-H atoms in the best least-squares structural fitting of the organic molecules, calculated by the Kabsh's procedure [34] is 0.037 Å (0.018 Å excepting the ring halogen atoms) and involves an improper relative rotation (determinant equal to -1) around the common molecular centroid. Figure 5 is an ORTEP [31] drawing of the chlorine-containing crystal. The corresponding intra-molecular bond distances and angles for both compounds are listed in the Supplementary Material, Tables S1b,c.

Due in part to delocalized π-bonding, the 5-X-2-hydroxyphenylidene (X=Cl, Br) fragments are nearly planar [*rms* deviation of non-H atoms from the best least-squares plane is less than 0.035 Å for (**3**) and 0.036 Å for (**4**)]. As shown in Fig. 5, the planarity affords the formation of an intra-molecular OH···N bond [OH···N bond distances of 2.002 Å (**3**) and 2.064 Å (**4**), O-H···N angles of 147.2º (**3**) and 145.41º (**4**)]. As expected, the positively charged pyridine moiety is also planar [*rms* deviation of atoms from the plane of 0.015 Å (**3**), 0.014 Å (**4**)] and therefore the only degrees of freedom left to define the molecular conformation are un-hindered rotations around the C1-C8, N1-N2, N2-C9, and C9-C10 σ-bonds. In fact, the chiral organic conformers are related to each other mainly through a change of 32.9(3)º in the torsion angle around C9-C10 bond.

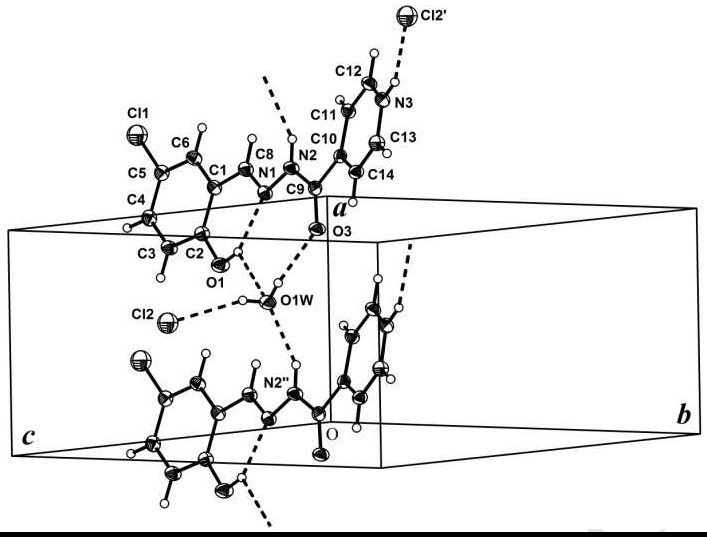

Figure 5. View of the chlorine-containing member of the (E)-N'-(5-X-2-hydroxybenzaldehyde)isonicotinohydrazide (X: Cl, Br) chloride hydrate isomorphic pair (**3**) and (**4**).

Observed intra-molecular bond distances and angles are in agreement with the Organic Chemistry's rules. In particular, C-C distances within the phenyl ring [in the 1.368(4)-1.414(4) Å (**3**) and 1.375(4)-1.402(4) Å (**4**) ranges] are as expected for phenyl resonant-bond structures. C-X bond distances are 1.743(3) Å (**3**) and 1.901(3) Å (**4**). The short imino C8-N1 length [1.267(4) Å (**3**) and 1.268(4) Å (**4**)] contrasts with the longer amido C9-N2 value [1.339(4) Å (**3**) and 1.345(4) Å (**4**)], clearly confirming the formally double and single bond character for these links, respectively. The distance of N-N single bond linking the 5-X-2-hydroxyphenylidene and pyridincarbonylic molecular fragments is 1.388(3) Å (**3**) and 1.396(3) Å (**4**). C-OH and C=O bond distances of 1.349(4) Å (**3**) and 1.355(4) Å (**4**), and 1.223(4) Å (**3**) and 1.217(4) Å (**4**) are the expected for the single and double character of these bonds, respectively. C-N bond lengths within the pyridinum group are 1.340(4) and 1.330(4) Å (**3**), and 1.336(4) and 1.329(4) Å (**4**). Bond distances in the bromide-containing organic cation are in general agreement with the corresponding ones reported in the literature for the neutral (deprotonated) moiety [35, 36].

The crystals are further stabilized by (pyr)$NH^+\cdots$Cl and OwH$\cdots$Cl bonds. The water molecule also bridges neighboring organic molecules acting as donor in a OwH$\cdots$O(carb) bond and as acceptor in a PhOH$\cdots$Ow bond with a given organic molecule and as acceptor in a NH$\cdots$Ow bond with another one (see Figure 5). Hydrogen bond distances and angles for both compounds are detailed in the Supplementary Material, Tables S2b,c.

3.2. Conformational analysis and geometry optimization

As it was previously mentioned, calculations were done using M06-2X functional and 6-311G(d,p) basis set in the gas phase and including solvent effects, as described in the experimental section.

In the case of (**1**), the conformational searching shows that one structure is more stable than other conformations by more than 4 kcal mol^{-1}, both in the gas phase and after including solvent effects. Even the conformation optimized from the X-ray structure is found to be well above in energy than the lowest-energy conformation. For (**3**), the conformational searching in the gas phase shows that one conformation is more stable than other conformations by about 3 kcal mol^{-1}, whereas the conformation optimized from the X-ray structure becomes the more stable one by about 1 kcal mol^{-1} after including solvent effects. Interestingly, (**4**) exhibits a very similar behavior. A conformation is more stable than others by more than 1 kcal mol^{-1} in the gas phase, whereas the conformation optimized from the X-ray structure becomes the more stable one by about 2 kcal mol^{-1} when solvent effects are taken into account. Finally, in the case of (**2**), for which no experimental structure is known, the conformational searching leads to optimized geometries that become the more stable ones by more than 3 kcal mol^{-1} both in the gas phase and after including solvent effects. From now on, the lowest-energy conformations obtained after including solvent effects are used both for the comparison of geometrical parameters with those structures obtained by X-ray diffraction methods and for the calculation of electronic transitions that aid in the assignment of the electronic spectra. On the other hand, gas-phase lowest-energy conformations are used to calculate harmonic vibrational frequencies that are useful in the assignment of experimental vibrational spectra.

A selection of calculated geometrical parameters is listed in Table 2. Experimental values for those structures that were characterized by X-ray diffraction methods and structural data calculated for (**2**) are included for comparison. It is appreciated from the table that the intra-molecular N1···HO1 bond is overestimated by the calculations in both salicylaldehyde derivatives (**3**) and (**4**). In addition, C-H distances are also slightly overestimated by the calculations. Nonetheless, there is excellent agreement between experimental and theoretical results regarding C-O, C-Cl and C-Br bond distances. It is worth noting that interatomic distances obtained by optimizing with solvent effects for (**2**) agree very well with those obtained for (**1**)

and that C-Br bond distance in (**2**) shows almost the same value as the ones found both experimentally and theoretically for (**4**). Calculated bond and torsion angles are also in agreement with those obtained by X-ray diffraction methods and calculated values for (**2**) are very close to those obtained for the other hydrazones. Regarding bond angles, calculated values are in excellent accordance with experimental results (see Table 2). It is worth noticing that the angle formed by –OH with the oxygen atom from OCH_3 substituent in vanillin derivatives, is well reproduced by calculated results, being also very close to the value found in (**2**) compound, for which there is no experimental structural data. Also, in salicylaldehyde derivatives, O-H···N1 and C2-O-H bond angles are well reproduced by calculated results, in accordance with the inter-molecular hydrogen bond between N1 and the OH group. Torsion angle values obtained by DFT methods and, in particular, those involved in these inter-molecular hydrogen bonds, show a good agreement with those obtained by diffraction experiments.

Table 2. Selected experimental and calculated (M06-2X/6-311G(d,p)) structural parameters. See Figures 3-5 for atom labeling and substituents nature. For compound (**1**), experimental data in the first column were extracted from Ref. 6.

	INHVa (1)			**INHBrVa (2)**	**INHClSal (3)**		**INHBrSal (4)**	
	Exp.[a]	Exp.[b]	Calc.	Calc.	Exp.	Calc.	Exp.	Calc.
				Bond lengths (Å)				
N1···HO1	---		---	---	2.015	1.801	2.024	1.804
C2-R4	0.929	1.046	1.085	1.082	1.349	1.345	1.356	1.353
C3-R3	1.367	1.362	1.367	1.363	0.930	1.084	0.930	1.083
C4-R2	1.358	1.365	1.369	1.358	0.930	1.083	0.930	1.083
C5-R1	0.930	0.999	1.084	1.900	1.743	1.749	1.901	1.890
C13-N3	1.321	1.326	1.335	1.334	1.330	1.346	1.330	1.346
				Bond angles (°)				
O-H-N1 (R4)	---	---	---	---	147.2	142.5	143.7	142.5
C-O-C3 (R3)	116.9	117.0	122.3	123.5	---	---	---	---
C2-O-H (R4)	---	---	---	---	107.3	109.3	107.8	109.4
C4-O-H (R2)	110.9	111.1	113.6	112.0	---	---	---	---
O-H (R2)-O(R3)	111.8	107.9	112.1	103.6	---	---	---	---
C1-C2-R4	120.1	120.1	120.8	121.1	123.1	123.1	123.3	123.1
C2-C3-R3	125.5	125.0	113.3	113.1	119.4	118.4	119.3	118.4

C3-C4-R2	121.4	122.8	127.3	126.3	120.2	120.3	120.6	120.1
C4-C5-R1	120.0	117.8	116.7	118.0	119.7	119.5	119.0	119.9
				Torsion angles (°)				
C14-C10-C9-N2	174.1	6.69	-143.5	-141.9	163.9	140.2	-163.2	-142.1
C10-C9-N2-N1	175.5	-179.5	10.7	10.7	-177.5	-180.0	177.4	179.8
N2-N1-C8-C1	-178.3	179.6	-180.0	-179.7	-176.0	179.9	175.3	178.6
N1-C8-C1-C6	-170.5	-4.53	4.50	0.918	177.3	178.1	-177.9	-178.8
C3-C2-O-H	---	---	---	---	-176.6	-179.1	-179.9	179.7
C5-C4-O-H	178.1	-178.7	-178.6	178.3	---	---	---	---
C2-C3-O-C	11.8	-3.03	-177.4	-179.9	---	---	---	---

3.3. Vibrational spectroscopy

The infrared spectra of the compounds were measured in the 400-4000 cm^{-1} spectral range. The assignments were accomplished with the help of data obtained from Density Functional Theory calculations at the M06-2X/6–311G(d,p) level using both visualization tools and potential energy distribution analyses, taking into account the internal coordinates that mainly contribute to each calculated frequency. Recorded spectra of INH, Va and (**1**) in the most relevant spectral range, namely 1800-400 cm^{-1}, are depicted in Figure 6. IR spectra of (**2**), (**3**) and (**4**) are included as Supplementary Material. (Figures S1a-S1d). The analyses based on the potential energy distribution are available as Supplementary Material.

In order to illustrate the behavior in the high frequencies spectroscopic region, FTIR spectra of one hydroxialdehyde (**Va**) and one hydrazone showing protonated pyridine N atom (**3**) in the 4000-400 cm^{-1} range, are included as Supplementary Material (Figures S1-e and S1-f, respectively)

A selection of relevant vibrational modes denoting the formation of the hydrazones are listed in Table 3, together with calculated values and proposed assignments. The complete list of vibrational modes and assignments are available as Supplementary Material Tables S3a-S3e. The assignments are in agreement with data reported previously [2,3,6-8,34,37]. Results for the already previously reported hydrazone from INH and o-vanillin (INHoVa) [2] are included in the Table for the purpose of comparison. For atom numbering in the following discussion see Figure 3.

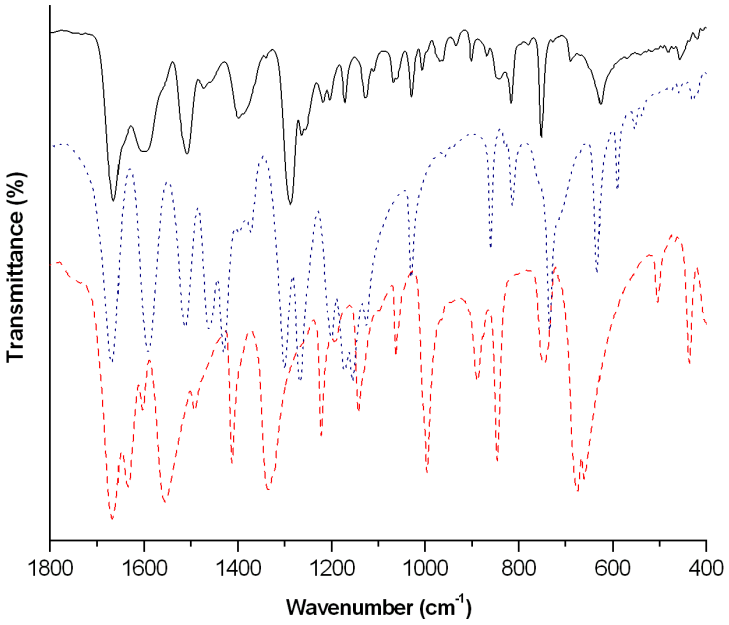

Figure 6. Experimental IR spectra of INH (red, dashed), Va (blue, dotted) and INHVa (**1**) (black, solid) in the 1800–400 cm^{-1} spectral range.

Table 3. Selected experimental bands of the studied Schiff bases IR spectra. Values for INH and the respective aldehydes are included for comparison. Complete assignment of relevant bands and calculated frequencies are available as Supplementary Material (Tables S3a-S3e).

Assignment	INH	o-HVa	INHoVa	Va	INHVa (1)	BrVa	INHBrVa (2)	ClSal	INHClSa (3)l	BrSal	INHBrSal (4)
ν OH		3014 w	3014 vvw	3018 w	3020 sh	3018 vw	3037 m	3047 vw	3048 w	3042 vw	3044 w
ν N(Py)H			2590 m,b		--		---		2517 m,b		2410 m,b
ν C=O	1667 vs	1645 vs	1688 vs	1665 vs	1665 vs	1676 vs	1676 s	1663 vs	1674 vs	1672 vs	1676 vs
ν C=N			1606 vs		1599 s,b		1598 s,b		1603 s,b		1605 vs,b
δ OH		1388 s	1392 sh	1430 s	1398 m	1426 s	1418 m	1378 s	1363 m,b	1373 m	1361 m-w
νAr-OH		1327 s	1324 m-w	1300 m	1287 s	1354 s	1297 s	1304 m	1301 m	1305 mw	1301 m
ν N-N	1192 vw		1148 w		1172 m-w		1188 m		1182 w,b		1197 vw
γ OH		838 m	839 m	813 m	816 m	854 s	840 w,b	831 s	836 m-s	892 m	834 m-s
γ NH	437 w		453 vw		456 vw		454 vw		448 vw		447 vw

Symmetrical and unsymmetrical νH_2O modes are found in similar frequencies in all the compounds. The Ar-X (X= Cl, Br) stretching modes appear around 500 cm^{-1} for the bromine Schiff bases, while for the chlorine Schiff base are located at 715 cm^{-1}.

N–H Vibrations

Stretching -NH vibrations of the hydrazone moiety (N2), appear in the range of 3209-3113 cm^{-1}, in agreement with the corresponding ones observed for INHoVa (3205 cm^{-1}).

It is found in the crystal structures of salicylaldehyde derivatives (**3**) and (**4**) that the pyridinic nitrogen is protonated. The broad intense band at 2517 cm^{-1} and 2410 cm^{-1}, respectively, observed for these Schiff bases can be assigned to the pyridinic N-H stretching mode. Regarding these results, we can propose that the band with similar shape at 2590 cm^{-1} in INHoVa spectra, corresponds to this mode [5]. It is worth mentioning that Malhotra et al [37] report the (**1**) hydrazone protonated at the pyridinic nitrogen. Despite this fact, they do not report N-H vibrations.

Unsurprisingly, the bands related to the NH_2 group in INH (at 3111, 1634 and 1321 cm^{-1}) are not present in the hydrazones spectra. A very weak band, corresponding to NH(hyd) out-of-plane deformation (γ) is found between 447 cm^{-1} and 456 cm^{-1}. The NH bending mode is found to be coupled with other modes in the hydrazones studied here and in INHoVa, showing a non-distinctive tendency along the family of compounds.

N-N stretching band, on the other hand, appears between 1172 cm^{-1} and 1197 cm^{-1} for the studied compounds, while for INHoVa and INH is at 1148 cm^{-1} and 1192 cm^{-1}, respectively.

O–H Vibrations

The IR spectra of the studied compounds show weak bands corresponding to OH stretching modes in the 3020-3048 cm^{-1} range. Values obtained from DFT methods are much higher than the experimental ones as H-bond interactions, present in the crystal packing of the hydrazones and the aldehydes, are neglected in the calculations. This stretching vibration is observed at 3014 cm^{-1} in INHoVa Schiff base. It also remains observable at almost the same frequency after condensation for all compounds except (**2**).

Regarding δOH mode, it can be seen from the tables that it shifts to lower frequencies upon condensation for all Schiff bases. Notwithstanding, INHoVa compound shifts this mode to a higher value, from 1388 cm^{-1} in o-HVa to 1392 cm^{-1} in the hydrazone. With the aid of computational methods, it is also observed that this vibration is in general present in combination with other modes, making it difficult to analyze the trend in the frequency values.

Comparing the hydrazones Ar-OH stretching mode, including INHoVa, with the corresponding aldehyde, it can be appreciated from the table that it is conserved except for (**1**). This behaviour can be explained by the OH group position together with the presence of deprotonated pyridinic nitrogen atom. As can be seen in the packing of (**1**), the OH is linked to the referred N atom of a neighboring molecule by H-bond interactions, hence, leading to a red shift of this mode.

Moreover, as it was expected, computational methods underestimate OH out-of-plane deformation (γ), which is conserved in all cases, but shows a slight shift in both Va derivatives.

C=O and C=N stretching

The strong bands found from 1663 cm^{-1} to 1676 cm^{-1} are characteristic of the C=O stretching of the Schiff bases. It is seen that this mode is slightly blue-shifted in all the hydrazones, except for (1) in which is conserved.

A strong band is observed in the 1599–1605 cm^{-1} range, characteristic of the C=N stretching mode, which appears due to the formation of the hydrazone. Considering INHoVa [2] (C=N stretching band at 1606 cm^{-1}, see Table 3) and other related compounds [3], it can be inferred that this mode is insensitive to the nature and position of the substituents in the aldehyde ring.

In addition, it is observed that DFT calculations overestimate OH, C=O and C=N stretching modes, possibly due to the lack of restrictions in the gas phase that are present in the solid (see Supplementary Material). It must be noted that the hydrogen atom from the OH group, the oxygen atom of C=O moiety and the nitrogen atom of C=N group are all involved in H-bonds in the crystals (see Figures 4 and 5).

OCH_3 Vibrations

Ar-OCH_3 stretching vibrations are present as broad bands in vanillin derivatives. For (**1**) it appears at 1254 cm^{-1} and for (**2**) from 1250 cm^{-1} to 1264 cm^{-1}, coupled with other modes. It is worth mentioning that INHoVa compound has similar bands in the 1256-1283 cm^{-1} range.

Regarding CH_3 vibrations, the asymmetrical δCH_3 strong band is observed at 1510 cm^{-1} in (**1**) and at 1498 cm^{-1} in (**2**), being both in agreement with the value of 1464 cm^{-1} found for INHoVa. In the three compounds, this band is accompanied by a weak band in the 1440 cm^{-1}- 1471 cm^{-1} range, corresponding to the symmetrical mode.

C–H Vibrations

The IR spectra of the compounds show weak bands corresponding to C8H stretching vibrations between 2842 cm^{-1} and 2926 cm^{-1} in the Schiff bases. These modes appear shifted to lower frequencies in comparison with those of the aldehydes, in most cases, except for INHoVa. Calculations overestimate frequency values in all cases.

It is also seen that symmetric and antisymmetric CH(methyl) stretching vibration modes are conserved in all hydrazones after condensation, in comparison with the same mode of the aldehyde. Calculated values of these stretching frequencies are higher than the observed ones. It is worth mentioning that these modes have a similar behaviour than those of INHoVa.

The band assigned to rings ν CH modes appear in the 3157-3050 cm^{-1} region in INHoVa; 3156-3046 cm^{-1}region in (**1**); 3148-3094 cm^{-1} region in (**2**); 3089-3027 cm^{-1} region in (**3**) and in the 3091-3017 cm^{-1} region in (**4**). It is worth noticing that for Va derivatives, the highest frequency value is originated in the aldehyde fragment, contrary to the salicylaldehyde derivatives, in which it corresponds to the INH fragment of the molecules. It is observed that the bands related to the C-H stretching mode in the hydrazide fragment are blue-shifted in comparison with those of INH. The bands corresponding to CH stretching modes in the aldehydes are overlapped with broad bands due to H_2O stretching in some cases (see Tables S3a-S3e). As a consequence, a comparison between these modes and those of the hydrazones could not be made.

3.4. NMR spectroscopy

^{1}H NMR and^{13}C NMR spectra of (**2**), (**3**) and (**4**) were registered as DMSO-d6 solutions (see experimental section for detailed information). Selected spectral data and their assignments are listed in Table 4, together with previously reported INHoVa and (**1**) data [2, 37]. Recorded spectra of compound (**4**), for which no crystal structure has been determined, are shown in Figure 7. It can be seen, with more clarity in the ^{1}H spectrum, that signals have satellite weaker ones that conserved the ratio of integrated area with respect to the main signals. This fact could be a consequence of tautomeric equilibrium in solution.

Table 4. Selected ^{1}H and ^{13}C (500 MHz) NMR chemical shifts, in ppm, for the Schiff bases (d_6-DMSO). Calculated chemical shifts and data reported by other authors are also shown.

	INHoVa		**INHVa (1)**		**INHBrVa (2)**		**INHClSal (3)**		**INHBrSal (4)**	
	Exp. [2]	**Calc. [2]**	**Exp. [37]**	**Calc.**	**Exp.**	**Calc.**	**Exp.**	**Calc.**	**Exp**	**Calc.**
H-O	12.46	11.56	5.08	6.15	4,92	6.50	12.98	11.48	12.95	10.78
H-C=N	8.76	8.91	8.34	8.12	8.50	7.98	8.81	8.60	8.81	8.45
H-N	---	12.48	---	---	---	---	11.07	11.26	11.11	11.21
C=N-H	10.70	10.30	11.86	8.71	12.68	8.74	8,98	9.51	9.05	9.10
					^{13}C					
C=O	160.10	167.4	163.42	175.52	159.84	175.48	160.09	166.50	159.81	166.00
O-CH_3	55.87	57.19	55.89	58.67	55.99	59.05	---	---	---	---
C-OH	148.00	158.00	151.94	158.4|	148.97	154.83	155.59	168.55	156.6	166.27

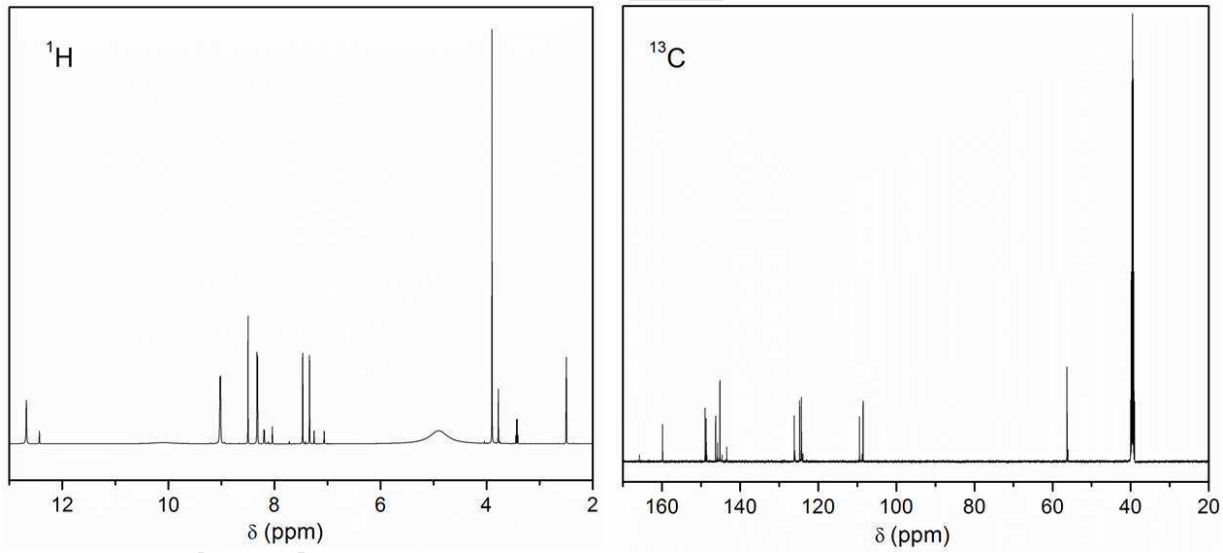

Figure 7: ^{1}H NMR (a) and ^{13}C NMR (b) of INHBrVa (**2**) in d_6-DMSO solution

The spectra of the hydrazones showed a signal at δ 4,92 -12.95 ppm characteristics of phenolic OH proton, sensitive to their position in the ring. Calculations underestimate these chemical shifts for (**3**) and (**4**) hydrazones in wich OH···N H-bonds give rise to pseudo-rings. On the contrary, values for (**1**) and (**2**) having the OH group in *para*-possiton, are overestimated. This could be explained by considering that calculations were done for a static conformation, while in solution atoms can freely rotate along a single bond and thus, observed chemical shifts are average values

of different conformations. A singlet observed at δ 8.50-8.81 ppm is assigned to the azomethine proton. The signals at δ 8.98-12.68 ppm are proposed to be due to the C=N-H hydrazine protons. Different values observed in the protonic spectra are proposed to be due to the variation of substituents in the hydrazone's rings and to the effect of protonation or deprotonation of the pyridinic N in the molecules. It is interesting to see that despite the fact that Malhotra et al [37] report the hydrazone to be protonated in the pyridinic nitrogen, the authors do not report the respective signal in the ^{1}H NMR spectrum. In the case of (**3**) and (**4**) a very broad signal of difficult evaluation at δ 11 ppm approximately, can be assigned to this proton.

Besides the selected signals listed in the table, two well-defined aromatic spin systems can be observed. As expected, pyridine hydrogens appear at higher δ values than those of the phenolic ring.

Regarding the ^{13}C spectra, the presence of a peak at δ 159.81-160.1 ppm is assigned to the carbonyl carbon. The methoxy carbon is proposed to show a signal at 55.89 ppm for (**1**) and at 55.99 ppm for (**2)**, both vanillin derivatives, in agreement with the reported for *o*-vanillin derivative at δ 55.87 ppm. The carbon atom linked to the OH group is, as Table 4 shows, in the 148.0-156.60 ppm range. Calculations were of aid to the assignment of the ^{13}C chemical shieldings, despite the fact that they generally overestimate values of the carbon spectra.

3.5. Electronic Spectroscopy

3.5.1. Spectra analysis

The electronic absorption spectra of INH, hydroxy-aldehydes and of the hydrazones were measured in the 200-800 nm spectral range. Figure 8 shows the electronic spectrum of the hydrazones in the most relevant spectral range, as an illustrative example. INHoVa spectrum is included for comparison.

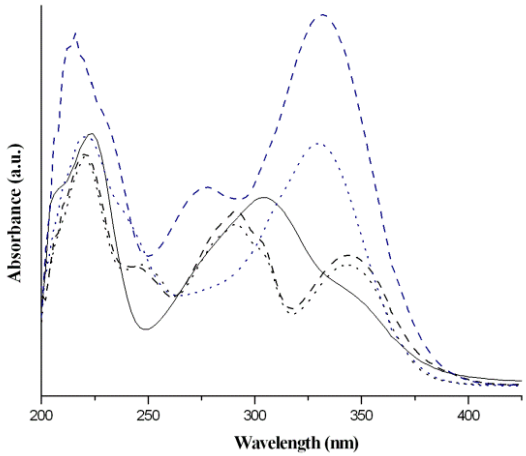

Figure 8. Electronic absorption spectra of the hydrazones in ethanolic solution: INHVa (**1**): dashed, blue; INHBrVa (**2**), dotted, blue; INHoVa, solid black; INHClSal (**3**), dashed black and INBrSal (**4**) dotted black.

The studied Schiff bases contain two aromatic rings, one belonging to the INH and the other to the aldehyde. For simplicity, the descriptions of the electronic transitions involving these rings are done mentioning INH or ALD referring to the respective fraction of the molecule.

Experimental absorption bands and calculated electronic transitions are listed in Table 5, together with the proposed assignments. Only those calculated electronic transitions relevant for the assignments are listed. The MO's mainly involved in the electronic transitions used to assign observed bands are available as Supplementary Material (Figures S2a-d). It can be seen from Table 5 that the calculated transitions describe very well the experimental electronic spectra.

Table 5. Electronic absorption spectra of 3 x 10^{-5} M ethanolic solutions of the studied isonicotinoyl hydrazones. Results from TD-DFT are also shown. Percentage contributions of calculated transitions are given in parentheses. Absorption maxima are given in nm. Oscillator strengths, shown in parenthesis, are in a.u.

INHVa (1)		
Exp.	**Calc.**	**Assignment**
208 sh	210 (0.0485)	HOMO – 4 → LUMO + 1 (72%)
214	215 (0.1011)	HOMO – 1 → LUMO + 4 (61%)
232 sh	240 (0.6052)	HOMO → LUMO + 4 (31%) HOMO – 1 → LUMO + 1 (55%)

276	280 (0.2491)	HOMO – 1 → LUMO (58%)
	289 (0.1193)	HOMO → LUMO + 1 (85%)
332	328 (0.3620)	HOMO → LUMO (98%)

INHBrVa (2)

Exp.	Calc.	Assignment
210 sh	215 (0.0802)	HOMO – 3 → LUMO + 1 (34%)
		HOMO – 1 → LUMO + 2 (34%)
222	219 (0.1027)	HOMO – 4 → LUMO + 1 (29%)
		HOMO – 3 → LUMO + 1 (23%)
	235 (0.1369)	HOMO – 1 → LUMO + 1 (23%)
		HOMO → LUMO + 1 (20%)
	240 (0.2914)	HOMO → LUMO +2 (33%)
242 sh		HOMO – 3 → LUMO (20%)
	241 (0.1885)	HOMO → LUMO + 2 (56%)
307 sh	278 (0.2373)	HOMO – 1 → LUMO + 1 (88%)
330	316 (0.4116)	HOMO → LUMO (98%)

INHClSal (3)

Exp.	Calc.	Assignment
210 sh	210 (0.1039)	HOMO – 2 → LUMO + 3 (20%)
220	231 (0.3940)	HOMO → LUMO + 3 (76%)
246	245 (0.0265)	HOMO – 3 → LUMO (84%)
292	260 (0.4151)	HOMO – 1 → LUMO + 1 (83%)
303 sh	307 (0.1913)	HOMO → LUMO + 1 (93%)
345	404 (0.1661)	HOMO → LUMO (98%)

INHBrSal (4)

Exp.	Calc.	Assignment
208 sh	212 (0.2034)	HOMO – 1 → LUMO + 3 (39%)
		HOMO → LUMO + 6 (38%)
220	234 (0.4460)	HOMO → LUMO + 3 (76%)
248	239 (0.1112)	HOMO – 6 → LUMO (63%)
291	260 (0.4147)	HOMO – 1 → LUMO + 1 (83%)
304 sh	308 (0.1668)	HOMO → LUMO + 1 (94%)
344	407 (0.1580)	HOMO → LUMO (98%)

sh = shoulder

3.5.2. Description of the MO's involved in the transitions

For all hydrazones (see Figures S2a-S2d), HOMO and HOMO–1 are π in character in the aldehyde ring, and non-bonding in the OH, C-N, C=O and C=N groups. In addition, they have some contributions from the different electrophilic substituents of the aldehydes, namely OCH_3

(**1**), Br [(**2**) and (**4**)] and Cl (**3**). HOMO–2 in (**3**) is non-bonding in Cl atom, the hydrazone group and oxygen atoms; it is also π in character in both INH and ALD rings. HOMO–3, involved in electronic transitions of (**2**) and (**3**), is π in character in the aldehyde ring for the salicylaldehyde derivative and in INH ring for the vanillin derivative; it is also located in oxygen and halogen atoms, C=N and C-N groups. HOMO–4 is involved in electronic transitions of (**1**), (**2**) and (**4**). In (**1**) is π in character in the aldehyde ring and it is also located in oxygen atoms, pyridinic nitrogen and hydrazone group. In (**2**), is π in character in the INH ring with some contributions from nitrogen and oxygen atoms of C=N and C=O groups. In (**4**), it is distributed among the Br atom, oxygen atoms and the hydrazone group; it is also π in character in the rings, mostly INH ring, being very similar to HOMO–6.

The LUMO is mostly π anti-bonding in the INH ring for the four hydrazones; with some contributions from oxygen atoms of the C=O group, atoms in the hydrazone moiety and ALD ring. LUMO+1 is similar to LUMO, but involving also oxygen atoms from the OCH_3, the OH group and the aldehyde ring. LUMO+2 is involved in electronic transitions of (**2**), it is π* in character in both rings and it is also localized in Br atom and O atom of OCH_3 substituent. LUMO+3, on the other hand, participates in electronic transitions of salycilaldehyde derivatives, (**3**) and (**4**). It is π* in character in ALD ring and non-bonding in the halogen atom, O atom of OH group and C (8). LUMO+4 is π* in character in ALD ring of (**1**). LUMO+6 is π* in character in both rings, with some contributions from C-N, C=N and C=O groups of (**4**).

3.5.3. Electronic absorption spectrum of INHVa (1)

According to the above description and the data from Table 5, the observed shoulder at 208 nm is calculated at 210 nm and mainly assigned to a π → π* transition from ALD ring to the INH ring. The observed band at 214 nm, which is calculated at 215 nm, is proposed to be due to a transition involving ALD ring, with some contributions of C-N and C=N groups. A π → π* electronic transition mainly from ALD ring to INH ring and with minor contributions from C=N, C=O and OH groups is calculated at 240 nm to describe the observed shoulder at 232 nm. Two close electronic transitions calculated at 280 nm and 289 nm, correspond to the band measured at 276 nm; this band is due to π → π* transitions from the ALD fragment of the molecule to the INH

one, involving also OH, C-N, C=N and OCH_3 groups. The band observed at 332 nm is calculated at 328 nm and assigned mostly to a $\pi \rightarrow \pi^*$ transition from ALD ring to the INH ring.

3.5.4. Electronic absorption spectrum of INHBrVa (2)

The bands are assigned on the basis of the description of the MO's and the data of Table 5. The shoulder observed at 210 nm is calculated at 215 nm and assigned mostly to a $\pi \rightarrow \pi^*$ transition involving INH ring with minor non-bonding contributions from Br atom, oxygen atoms and C-N and C=N groups. The band at 222 nm is described by two calculated transitions, one at 219 nm and the other at 235 nm; it is assigned to $\pi \rightarrow \pi^*$ transitions from both aromatic rings to INH ring. The shoulder at 242 nm is also described by two calculated values, at 240 nm and at 241 nm; it is assigned to $\pi \rightarrow \pi^*$ transitions involving both rings, with minor contributions from the electrophilic substituents of the aldehydes. The shoulder found at 307 nm and the band at 330 nm are calculated at 278 nm and 316 nm, respectively. These bands are assigned to $\pi \rightarrow \pi^*$ transitions from ALD ring to the INH ring, with minor contributions from OH, C-N, C=O and C=N groups.

3.5.5. Electronic absorption spectrum of INHClSal (3)

On account of the provided descriptions of the MO's and the electronic spectra described in Table 5, the shoulder observed at 210 nm is mainly assigned to an electronic transition from both rings of (**3**) to the ALD fragment of the molecule, including non-bonding contributions of its susbtituents. The band at 220 nm is calculated at 231 nm and assigned to a $\pi \rightarrow \pi^*$ transition in the ALD ring and its substituents. The band at 246 nm is due to a $\pi \rightarrow \pi^*$ transition from ALD ring to INH ring, with some contributions of nitrogen and chlorine atoms. The band at 292 nm and the shoulder at 303 nm are calculated at 260 nm and 307 nm, respectively; they are assigned to electronic transitions from ALD ring to both rings with contributions from Ar-C, C-N and C=N bonds. Interestingly, chlorine atom is not involved. The band measured at 345 nm is calculated at 404 nm and assigned to a $\pi \rightarrow \pi^*$ transition from ALD ring and substituents to INH ring, with minor contributions from C-N and C=N bonds, OH group and oxygen atom from C=O.

3.5.6. Electronic absorption spectrum of INHBrSal (4)

According to the analysis of the MO's and the data from Table 5, the shoulder at 208 nm can be mainly assigned to one transition in ALD ring and its substituents, with minor contributions from oxygen and nitrogen atoms; and to another from ALD ring to both rings, C and O atom from C=O group and nitrogen atom form hydrazone group. The band at 220 nm, calculated at 234 nm, is assigned to $\pi \rightarrow \pi^*$ transitions in ALD ring, with non-bonding contributions from bromine, oxygen and nitrogen atoms. The band found at 248 nm, is calculated at 239 nm and assigned to $\pi \rightarrow \pi^*$ transitions in both ALD and INH rings, with non-bonding contributions from bromine, oxygen and nitrogen atoms. The shoulders at 280 nm and 304 nm are assigned to transitions from ALD ring, including its substituents, to both rings with minor contributions from nitrogen atoms. The band at 291 nm is calculated at 293 nm and assigned mainly to a transition from both rings, bromine and oxygen atom from C=O, to INH ring. The band at 344 nm is described by two calculated values, one at 333 nm and the other at 407 nm; it is assigned to a $\pi \rightarrow \pi^*$ transition from ALD ring to INH ring, with minor contributions from bromine, nitrogen and oxygen atoms.

3.6 A theoretical analysis of the reactivity of the hydrazones

The interesting application of hydrazones as good chelating agents, has been extensively studied (see [1] and references therein). This capacity arises from the available electronic density in the –C=N-N-C=O group, suitable for metal coordination [5].

Furthermore, it has been stated before [38] that HOMO energies (E_H) are associated with the electron donating ability of a molecule. In particular, high values (that is, less negative ones) of E_H are likely to indicate a tendency of a molecule to donate electrons to appropriate receptors, such as transition metals. Thus, E_H could indicate the tendency of ligands to coordinate such metals.

On the other hand, the LUMO energy, E_L, is equivalent to electron affinity, according to Koopmans' theorem [39]. Moreover, LUMO energies are also associated with electron transfer rates [38]. Regarding the well-known anti-oxidant properties of this kind of ligands, often enhanced upon metal complex formation, the analysis of the electron affinity gains interest. This property has been employed to account for the electron transfer rate from superoxide anion to

copper atom [40-42]. The lower the electron affinity (that is, less negative values of E_L), the higher the electron transfer rate, leading to higher superoxide radical scavenging activity, being the superoxide dismutase-mimic activity one of the main interests in this kind of copper complexes. To gain more insight into the reactive behaviour of this family of hydrazones, we calculated these properties, which are listed in Table 6.

Table 6. HOMO (E_H) and LUMO (E_L) energies (in eV) for the hydrazones, calculated at the M06-2X/6–311G(d,p) level of theory.

	$\mathbf{E_H}$	$\mathbf{E_L}$
INHVa (1)	-6.49	-1.05
INHBrVa (2)	-7.31	-1.45
INHClSal (3)	-6.70	-3.11
INHBrSal (4)	-6.70	-3.11

It can be seen in Table 6 that the E_H values of the vanillin hydrazone, (**1**), and the salicylaldehyde derivatives (**3**) y (**4**) are the less negative ones and, moreover, they are close each other. Thus, they would be better candidates to form complexes with metal ions than the hydrazine (**2**). It is interesting to note from Figures 2 and 3 that the OH group is in *para* position in vanillin derivatives, whereas it is in *ortho* position in the salicylaldehyde derivatives. The OH group in *ortho* position, together with the azomethine group, might favour the role of polydentate chelating agent for salicylaldehyde derivatives. Therefore, it is proposed that (**3**) and (**4**) hydrazones would be better candidates to form complexes with metal ions than (**1**) or (**2**). Therefore, we propose that hydrazones (**3**) and (**4**) would have a better chance of being chelated than (**1**) or (**2**).

Calculated E_L values, shown in Table 6, indicate that (**1**) would have the highest superoxide radical scavenging activity of the studied hydrazones, closely followed by (**2**).

MEP-derived atomic charges (ESP charges, from now on) can be a useful index to identify potential sites for coordination with metals, as they predict possible sites for nucleophilic or electrophilic attacks [43]. We calculated them, in an attempt to identify these reactivity sites, as we have already done in previous work [44]. Selected ESP charges of the compounds are listed in

Table 7.

Table 7. MEP-derived atomic charges of selected atoms, in units of |e|, at the M06-2X/6–311G(d,p) level of theory. See Figure 3 for atom numbering and structures.

	INHVa (1)	**INHBrVa (2)**	**INHClSal (3)**	**INHBrSal (4)**
O (OH)	-0.5029	-0.5029	-0.5691	-0.5680
O (OCH_3)	-0.2436	-0.2497	------	------
N1	-0.2285	-0.1780	-0.1393	-0.1265
N2	-0.3222	-0.3453	-0.4125	-0.4131
N3	-0.6601	-0.6379	-0.1761	-0.1534
O (C=O)	-0.5134	-0.5057	-0.4591	-0.4572
Br1	------	-0.0307	------	-0.0196
Cl1	------	------	-0.0679	------

It can be seen from the table that the oxygen atoms belonging to OH and C=O groups present large negative ESP charges for all the molecules under study suggesting that they are prone to undergo electrophilic attacks. It is interesting to note that although the oxygen atom in the OCH_3 group exhibits a small negative ESP charge, it could participate in the coordination sphere of a complex together with the oxygen atom from the OH group, as it was determined in the vanillin-copper complex [45]. Also, both nitrogen atoms in the –C=N-N-C=O moiety seem to be good candidates for an electrophilic attack, although N2 presents a considerably most negative ESP charge than N1. As expected, N3 shows a small negative charge when is protonated in ClSal and BrSal Schiff bases, whereas large negative charges are found for that atom in (**1**) and (**2**), in which it is not protonated. The pyridinic nitrogen atom could participate in a coordination compound, forming complex structures, as it was reported previously [46]. These findings agree with those found above when the magnitude of E_H was correlated with the ability of the molecules under study to form complexes.

4. Conclusions

Four hydrazones derived from isoniazid (INH), a well-known antituberculous agent, were prepared. They were obtained with good yield upon condensation with a group of

hydroxybenzaldehydes, namely *Va, BrVa, ClSal, BrSal*.

The crystal structures of three of them were determined and compared with reported data for the related Schiff base INHoVa. Hydrazones (**3**) and (**4**) are isomorphic and chiral counterparts of each other. Structure of compound (**1**) differs from the already reported by other authors, probably as an effect of the crystallization rate during the synthesis process.

DFT-based calculations carried out on the family of compounds showed a very good agreement with experimental data. These results were of relevance in the interpretation and assignment of the bands in the spectroscopic analysis. The few cases in which the calculated values differed significantly from the experimental results were attributed to molecular interactions which were neglected in the calculations. Moreover, calculated geometrical parameters are in very good agreement with experimental data, even in the cases involving atoms that participate in intermolecular H-bonds.

The FT-IR of solid samples and UV-vis of ethanol solutions spectra of the four hydrazones were recorded together with those of INH and the respective aldehydes. They were analysed and discussed in comparison with INHoVa hydrazone. The vibrational behaviour is in perfect accordance with the expected for azomethine moiety formation and the observed crystallographic details. Strong coupling among different modes was observed in the assignment of various bands.

The effect of the nature and location of substituent groups in the ring and of protonation or deprotonation of the pyridinic N atom are also evidenced in the ^{1}H and ^{13}C NMR spectra.

In the electronic spectra the bands predicted in the calculations for the hydrazones could be observed and assigned. In most cases, more than one electronic transition was involved in each signal.

The calculation of some reactivity properties indicate that the Schiff bases (**3**) and (**4**) are good candidates to act as polydentate ligands in the formation of coordination compounds. On the other hand, the vanillin hydrazone (**1**) shows the highest superoxide radical scavenging activity, calculated as the energy of the LUMO, which could be related to electron transfer processes present in superoxide radical anion dismutation.

Acknowledgments

This work was supported by CONICET (CCT-La Plata), UNLP and ANPCyT, Argentina. G.A.E., O.E.P., R.P.D. and A.C.G.B. are members of the Research Career of CONICET. The

authors thank Christian D. Alcívar León (CEQUINOR-CONICET-UNLP) for his help with the NMR spectra.

Supplementary Material

Experimental FT-IR spectra of INHoVa, INHBrVa (**2**), INHClSal (**3**) and INHBrSal (4), respectively, are presented in Figures S1a-S1d. FT-IR spectra of (**1**) and (**3)** in the 4000-400 cm^{-1} range are compared in Figure S1-e. Drawings of the occupied and unoccupied molecular orbitals involved in the electronic transitions of (**1**), (**2**), (**3**) and (**4**), respectively, are shown in Figs. S2a-S2d. Complete geometrical parameters are listed in Tables S1a-S1c. Hydrogen bond distances and angles are listed in Tables S2a-S2c. Complete assignments for the IR spectra are included in Tables S3a-S3e. Fractional coordinates and equivalent isotropic displacement parameters of the non-H atoms for the compounds are shown in Tables S4a-S4c. Atomic anisotropic displacement parameters are presented in Tables S5a-S5c. The position of hydrogen atoms are presented in Tables S6a-S6c for the compounds suitable for X-ray diffraction analysis studied in the present work. Crystallographic structural data have been deposited at the Cambridge Crystallographic Data Centre (CCDC). Enquiries for data can be direct to: Cambridge Crystallographic Data Centre, 12 Union Road, Cambridge, UK, CB2 1EZ or (e-mail) deposit@ccdc.cam.ac.uk or (fax) +44 (0) 1223 336033. Any request to the Cambridge Crystallographic Data Centre for this material should quote the full literature citation and the reference numbers CCDC 1047603 (INHVa), CCDC 1047601 (INHClSal) and CCDC 1047602 (INHBrSal). Potential energy distribution analyses are shown in Tables S7a-S7d. Figure S3 shows the numbering schemes used in the potential energy distribution analyses.

References

[1] X. Xu, I . Aprahamian, Chem. Soc. Rev., 43 (2014) 1963-1981.
[2] A.C. González-Baró, R. Pis-Diez, B.S. Parajón-Costa, N.A. Rey, J. Mol. Struct. 1007 (2012) 95–101.
[3] V. Ferraresi-Curotto, G.A. Echeverría, O.E. Piro, R. Pis-Diez, A.C. Gonzalez-Baró, Spectrochim. Acta Part A 137 (2015) 692-700.
[4] E.F. Oga, Int. J. Pharm. Pharm. Sci. 2 (2010) 55–58.
[5] D. Cook, Can. J. Chem. 39 (1961) 2009-2024.
[6] X.F. Shi, L. He, G.Z. Ma, C.C. Yuan, Acta Cryst. E 63 (2007) o1119.

[7] M.R. Maurya, S. Khurana, C. Schulzke, D. Rehder, Eur. J. Inorg. Chem. (2001) 779-788.
[8] R. Manikandan, P.Viswanathamurthi, M. Muthukumar, Spectrochim. Acta Part A 83 (2011) 297-303.
[9] CrysAlisPro, Oxford Diffraction Ltd. version 1.171.33.48 (release 15-09-2009 CrysAlis171.NET).
[10] G.M. Sheldrick, Acta Cryst. A 64 (2008) 112-122.
[11] H.D. Flack, Acta Cryst. A 39 (1983) 876-881.
[12] J.J.P. Stewart, J. Mol. Model. 13 (2007) 1173–1213. MOPAC2012; James J.P. Stewart, Stewart Computational Chemistry, Colorado Springs, CO, USA, 2012. http://OpenMOPAC.net.
[13] Y. Zhao, D.G. Truhlar, Theor. Chem. Acc. 120 (2008) 215–241.
[14] R. Krishnan, J.S. Binkley, R. Seeger, J.A. Pople, J. Chem. Phys. 72 (1980) 650–654.
[15] T. Clark, J. Chandrasekhar, P.V.R. Schleyer, J. Comput. Chem. 4 (1983) 294–301.
[16] V. Barone, M. Cossi, J. Phys. Chem. A 102 (1998) 1995-2001.
[17] M. Cossi, N. Rega, G. Scalmani, V. Barone, J. Comput. Chem. 24 (2003) 669-681.
[18] A. Dreuw, M. Head-Gordon, Chem. Rev. 105 (2005) 4009-4037.
[19] P. Elliott, F. Furche, K. Burke, Rev. Comp. Chem. 26 (2009) 91-165.
[20] C. Adamo, V. Barone, J. Chem. Phys. 110 (1999) 6158-6170.
[21] M.W. Schmidt, K.K. Baldridge, J.A. Boatz, S.T. Elbert, M.S. Gordon, J.H. Jensen, S. Koseki, N. Matsunaga, K.A. Nguyen, S.J. Su, T.L. Windus, M. Dupuis, J.A. Montgomery, J. Comput. Chem. 14 (1993) 1347–136,3. GAMESS-US version 1October 2010 (R1).
[22] J. R. Cheeseman, G.W. Trucks, T.A. Keith, M.J. Frisch, J. Chem. Phys. 104 (1996) 5497-5509.
[23] R. Ditchfield, J. Mol. Phys. 27 (1974) 789-807.
[24] K. Wolinski, J.F. Hinton, P.J. Pulay, J. Am. Chem. Soc., 112 (1990) 8251-8260.
[25] J. Tomasi, B. Mennucci, E. Cancès, J. Mol. Struct. THEOCHEM, 464 (1999) 211-226.
[26] Gaussian 03, Revision D.01, M.J. Frisch, G.W. Trucks, H.B. Schlegel, G.E.Scuseria, M.A. Robb, J.R. Cheeseman, J.A. Montgomery, Jr., T. Vreven, K.N.Kudin, J.C. Burant, J.M. Millam, S.S. Iyengar, J. Tomasi, V. Barone, B. Mennucci,M. Cossi, G. Scalmani, N. Rega, G.A. Petersson, H. Nakatsuji, M. Hada, M. Ehara,K. Toyota, R. Fukuda, J. Hasegawa, M. Ishida, T. Nakajima, Y. Honda, O. Kitao, H.Nakai, M. Klene, X. Li, J.E. Knox, H.P. Hratchian, J.B. Cross, V. Bakken, C. Adamo,J. Jaramillo, R. Gomperts, R.E. Stratmann, O. Yazyev, A.J. Austin, R. Cammi, C.Pomelli, J.W. Ochterski, P.Y. Ayala, K. Morokuma, G.A. Voth, P. Salvador, J.J.Dannenberg, V.G. Zakrzewski, S. Dapprich, A.D. Daniels, M.C. Strain, O. Farkas,D.K. Malick, A.D. Rabuck, K. Raghavachari, J.B. Foresman, J.V. Ortiz, Q. Cui, A.G.Baboul, S. Clifford, J. Cioslowski, B.B. Stefanov, G. Liu, A. Liashenko, P. Piskorz, I.Komaromi, R.L. Martin, D.J. Fox, T. Keith, M.A. Al-Laham, C.Y. Peng, A.Nanayakkara, M. Challacombe, P.M.W. Gill, B. Johnson, W. Chen, M.W. Wong,C. Gonzalez and J.A. Pople, Gaussian, Inc., Wallingford CT, 2004.
[27] A.R.J. Allouche, Comput. Chem. 32 (2011) 174–182.

[28] B.M. Bode, M.S. Gordon, J. Mol. Graph. Model. 16 (1998) 133–138.
[29] http://info.ifpan.edu.pl/~kisiel/vibr/vibr.htm
[30] Marvin 6.2.2, 2014, ChemAxon (http://www.chemaxon.com).
[31] L.J. Farrugia, J. Appl. Cryst. 30 (1997) 565.
[32] Z. Shafiq, M. Yaqub, M.N. Tahir, A. Hussain, M.S. Iqbal, Acta Cryst. E 65 (2009) o2899.
[33] X. Liu, X-F. Shi, Acta Cryst. E 63 (2007) o4807.
[34] W. Kabsch, Acta Cryst. A 32 (1976) 922–923.
[35] T. Sedaghat, M. Yousefi, G. Bruno, H. A. Rudbari, H. Motamedi, V. Nobakht, Polyhedron 79 (2014) 88-96.
[36] D.S. Yang, Acta Cryst. E 62 (2006) o3755.
[37] M. Malhotra, G. Sharma and A. Deep, A. Pol. Pharm.Drug Res. 69 (2012) 637-644.
[38] M. Behpour, S.M. Ghoreishi, N. Mohammadi, N. Soltani, M. Salvati-Niasari, Corros. Sci. 52 (2010) 4046–4057.
[39] T.A. Koopmans, Physica 1 (1933) 104-113.
[40] H.F. Ji, H.Y. Zhang, Chem. Res. Toxicol. 17 (2004) 471-475.
[41] H.F. Ji, H.Y. Zhang, Bioorg. Med. Chem. Lett. 15 (2005) 21-24.
[42] L. Shen, H.Y. Zhang, H.F. Ji, J. Mol. Struct. (THEOCHEM), 817 (2007) 161-162.
[43] P. Politzer, J.S. Murray, in: K.B. Lipkowitz, D.B. Boyd (Eds.), Reviews in Computational Chemistry, John Wiley & Sons, Inc., Hoboken, NJ, USA, 1991, Vol. 2 pp. 273-312
[44] V. Ferraresi-Curotto, G.A. Echeverría, O.E. Piro, R. Pis-Diez, A.C. Gonzalez-Baró, Spectrochim. Acta Part A 118 (2014) 279-286.
[45][40] B. Kozlevčar, B. Mušič, N. Lah, I. Leban, P. Šegedin, Acta Chim. Slov. 52 (2005) 40-43.
[46] S. Naskar, M. Corbella, A.J. Blake and S. Kumar Chattopadhyay, Dalton Trans. (2007) 1150-1159.

Supplementary Material. Tables

Table S1a. Bond lengths [Å] and angles [°] for (E)-N'-(4-hydroxy-3-methoxybenzylidene) isonicotinohydrazide hydrate.

Bond lengths		Bond angles	
C(1)-C(2)	1.380(5)	C(2)-C(1)-C(6)	119.3(3)
C(1)-C(6)	1.389(4)	C(2)-C(1)-C(8)	122.6(3)
C(1)-C(8)	1.466(4)	C(6)-C(1)-C(8)	118.1(3)
C(2)-C(3)	1.391(4)	C(1)-C(2)-C(3)	120.2(3)
C(3)-C(4)	1.382(4)	C(4)-C(3)-C(2)	120.8(4)
C(4)-O(1)	1.365(4)	O(1)-C(4)-C(3)	118.1(3)
C(4)-C(5)	1.390(5)	O(1)-C(4)-C(5)	123.0(3)
C(5)-O(2)	1.362(4)	C(3)-C(4)-C(5)	118.9(3)
C(5)-C(6)	1.384(4)	O(2)-C(5)-C(6)	124.9(3)
C(7)-O(2)	1.413(4)	O(2)-C(5)-C(4)	114.6(3)
C(8)-N(1)	1.279(4)	C(6)-C(5)-C(4)	120.5(3)
C(9)-O(3)	1.222(4)	C(5)-C(6)-C(1)	120.4(3)
C(9)-N(2)	1.342(4)	N(1)-C(8)-C(1)	121.2(4)
C(9)-C(10)	1.502(4)	O(3)-C(9)-N(2)	123.6(3)
C(10)-C(14)	1.379(4)	O(3)-C(9)-C(10)	120.1(3)
C(10)-C(11)	1.387(5)	N(2)-C(9)-C(10)	116.3(3)
C(11)-C(12)	1.379(4)	C(14)-C(10)-C(11)	117.9(3)
C(12)-N(3)	1.323(4)	C(14)-C(10)-C(9)	116.6(3)
C(13)-N(3)	1.325(5)	C(11)-C(10)-C(9)	125.5(3)
C(13)-C(14)	1.391(4)	C(12)-C(11)-C(10)	118.5(3)
N(1)-N(2)	1.396(3)	N(3)-C(12)-C(11)	124.5(4)
		N(3)-C(13)-C(14)	123.8(3)
		C(10)-C(14)-C(13)	118.7(4)
		C(8)-N(1)-N(2)	114.4(3)
		C(9)-N(2)-N(1)	118.3(3)
		C(12)-N(3)-C(13)	116.5(3)
		C(5)-O(2)-C(7)	117.2(3)

Table S1b. Bond lengths [Å] and angles [°] for (E)-N'-(5-chlorine-2-hydroxybenzaldehyde) isonicotinohydrazide.

Bond lengths		Bond angles	
C(1)-C(6)	1.386(4)	C(6)-C(1)-C(2)	118.3(3)
C(1)-C(2)	1.414(4)	C(6)-C(1)-C(8)	118.4(3)
C(1)-C(8)	1.454(4)	C(2)-C(1)-C(8)	123.2(3)
C(2)-O(1)	1.349(4)	O(1)-C(2)-C(3)	117.4(3)
C(2)-C(3)	1.390(4)	O(1)-C(2)-C(1)	123.0(3)
C(3)-C(4)	1.368(4)	C(3)-C(2)-C(1)	119.6(3)
C(4)-C(5)	1.390(5)	C(4)-C(3)-C(2)	121.2(3)
C(5)-C(6)	1.385(4)	C(3)-C(4)-C(5)	119.6(3)
C(5)-Cl(1)	1.743(3)	C(6)-C(5)-C(4)	119.9(3)
C(8)-N(1)	1.267(4)	C(6)-C(5)-Cl(1)	120.4(2)
C(9)-O(3)	1.223(4)	C(4)-C(5)-Cl(1)	119.7(2)
C(9)-N(2)	1.339(4)	C(5)-C(6)-C(1)	121.3(3)
C(9)-C(10)	1.509(4)	N(1)-C(8)-C(1)	123.6(3)
C(10)-C(14)	1.386(4)	O(3)-C(9)-N(2)	125.2(3)
C(10)-C(11)	1.401(4)	O(3)-C(9)-C(10)	120.3(3)
C(11)-C(12)	1.368(4)	N(2)-C(9)-C(10)	114.4(3)
C(12)-N(3)	1.340(4)	C(14)-C(10)-C(11)	118.5(3)
C(13)-N(3)	1.330(4)	C(14)-C(10)-C(9)	118.6(3)
C(13)-C(14)	1.370(4)	C(11)-C(10)-C(9)	122.8(3)
N(1)-N(2)	1.388(3)	C(12)-C(11)-C(10)	119.0(3)
		N(3)-C(12)-C(11)	120.3(3)
		N(3)-C(13)-C(14)	119.9(3)
		C(13)-C(14)-C(10)	119.9(3)
		C(8)-N(1)-N(2)	113.9(2)
		C(9)-N(2)-N(1)	121.4(2)
		C(13)-N(3)-C(12)	122.2(3)

Table S1c. Bond lengths [Å] and angles [°] for (E)-N'-(5-bromide-2-hydroxybenzaldehyde) isonicotinohydrazide.

Bond lengths		Bond angles	
C(1)-C(6)	1.390(4)	C(6)-C(1)-C(2)	118.4(3)
C(1)-C(2)	1.402(4)	C(6)-C(1)-C(8)	118.6(3)
C(1)-C(8)	1.450(4)	C(2)-C(1)-C(8)	122.9(3)
C(2)-O(1)	1.355(4)	O(1)-C(2)-C(3)	116.8(3)
C(2)-C(3)	1.391(4)	O(1)-C(2)-C(1)	123.5(3)
C(3)-C(4)	1.375(4)	C(3)-C(2)-C(1)	119.7(3)
C(4)-C(5)	1.389(5)	C(4)-C(3)-C(2)	121.4(3)
C(5)-C(6)	1.378(4)	C(3)-C(4)-C(5)	118.9(3)
C(5)-Br(1)	1.901(3)	C(6)-C(5)-C(4)	120.4(3)
C(8)-N(1)	1.268(4)	C(6)-C(5)-Br(1)	120.5(2)
C(9)-O(3)	1.217(4)	C(4)-C(5)-Br(1)	119.1(2)
C(9)-N(2)	1.345(4)	C(5)-C(6)-C(1)	121.2(3)
C(9)-C(10)	1.507(4)	N(1)-C(8)-C(1)	123.3(3)
C(10)-C(11)	1.391(5)	O(3)-C(9)-N(2)	125.2(3)
C(10)-C(14)	1.387(4)	O(3)-C(9)-C(10)	120.8(3)
C(11)-C(12)	1.368(4)	N(2)-C(9)-C(10)	114.0(3)
C(12)-N(3)	1.336(4)	C(11)-C(10)-C(14)	118.3(3)
C(13)-N(3)	1.329(4)	C(11)-C(10)-C(9)	123.4(3)
C(13)-C(14)	1.372(4)	C(14)-C(10)-C(9)	118.3(3)
N(1)-N(2)	1.396(3)	C(12)-C(11)-C(10)	119.3(3)
		N(3)-C(12)-C(11)	120.3(3)
		N(3)-C(13)-C(14)	119.6(3)
		C(13)-C(14)-C(10)	120.1(3)
		C(8)-N(1)-N(2)	113.9(3)
		C(9)-N(2)-N(1)	120.9(3)
		C(13)-N(3)-C(12)	122.2(3)

Table S2a. Hydrogen bond distances and angles in (E)-N'-(4-hydroxy-3-methoxybenzylidene) isonicotinohydrazide hydrate.

D-H	d(D-H)	d(H···A)	∠(D-H···A)	d(D···A)	A	Symmetry operation
N2-H2A	0.860	2.135	166.7	2.978	O1W	
O1-H1	0.979	2.237	108.0	2.701	O2	
O1-H1	0.979	1.806	149.6	2.697	N3	[x-3/2, -y+1/2, z+1/2]
O1W-H1W	0.855	1.997	168.2	2.840	O3	[-x+1/2, y-1/2, -z+3/2]
O1W-H2W	0.856	2.247	143.3	2.978	O1	[-x-1/2, y-1/2, -z+3/2]

Table S2b. Hydrogen bond distances and angles in (E)-N'-(5-chlorine-2-hydroxybenzaldehyde) isonicotinohydrazide chloride hydrate.

D-H	d(D-H)	d(H···A)	∠(D-H···A)	d(D···A)	A	Symmetry operation
N2-H2	0.860	2.035	153.20	2.829	O1W	[x+1, y, z]
N3-H3N	0.860	2.180	153.94	2.977	Cl2	
O1-H1	0.834	2.012	147.18	2.750	N1	
O1-H1	0.834	2.491	112.48	2.913	O1W	
O1W-H1W	0.775	2.400	159.64	3.138	Cl2	[-x-1/2, -y+2, z-1/2]
O1W-H2W	0.731	2.043	167.42	2.761	O3	

Table S2c. Hydrogen bond distances and angles in (E)-N'-(5-bromide-2-hydroxybenzaldehyde) sonicotino hydrazide chloride hydrate.

D-H	d(D-H)	d(H···A)	∠(D-H···A)	d(D···A)	A	Symmetry operation
N2-H2	0.860	2.023	152.41	2.813	O1W	[x-1, y, z]
N3-H3N	0.860	2.189	154.74	2.989	Cl2	
O1-H1	0.768	2.064	145.41	2.731	N1	
O1-H1	0.768	2.539	110.54	2.899	O1W	
O1W-H1W	0.810	2.360	167.45	3.155	Cl2	[-x+5/2, -y, z+1/2]
O1W-H2W	0.796	1.987	166.95	2.768	O3	

Table S3a. Complete assignment of the IR spectrum of INHOVA. Experimental and calculated frequencies. Data of INH and *o*-HVa are included for comparison.

INH	o-HVA	INHOVA	Calculated	Asignment
		3578 w		$\nu_{as}H_2O$
		3428 m		$\nu_{s}H_2O$
3304 m		3205 w	3492	νNH (hyd)
		2590 m,b	3513	νNH (Py)
3111 vs				νNH_2
		3157 w	3186	νCH (*o*-HVa)ip
	3088 vw	3088 m	3061	ν_{as} CH_3
	3069 vw		3173	νCH (*o*-HVa)op
3050 w			3198	νCH (INH) ip
3013 w			3197	νCH (INH)op
			3182	
			3179	
	3039 vw	3050 w		νCH (*o*-HVa)
	3014 w	3014 w	3594	νOH
		2984 vw	3133	ν_{as} CH_3
	2939 w	2947 vw	3022	νCH(C8)
	2884 w		2995	ν_{s} CH_3
	2839 w	2844 vw		νCH (C8)
1667 vs		1688 vs	1795	νC=O
	1645 vs			νC=O (*o*-HVa)
1634 s				δNH_2
1602 m		1636 w	1669	νring (INH) + νring (*o*-HVa)
		1606 vs	1689	νC=N
		1576 w	1614	νring (INH) + νring (*o*-HVa)
	1591sh	1564 m	1657	νring (*o*-HVa)
1556 s		1501 m	1641	δNH(Py)+ (νring +δCH) INH
1492 w				(δCH + δNH + νring) INH
	1471 m	1464 s	1482	$\delta_{as}CH_3$
	1455 s	1440 sh	1460	$\delta_{s}CH_3$
1412 s				(δCH + νring) INH
	1388 s	1392 sh	1338	δOH
	1367 sh	1374 m	1380	δCH (C8)
1334 s		1338 sh	1361	(δCH + νring) INH
1321 sh				ρ_{r}NH2
	1327 s	1324 m-w	1316	νAr-OH + δCH(ring + C8) *o*-HVa
		1283 m		
	1257 s	1256 vs	1284	νAr-OCH_3 + δCH(ring) + δOH(phenol)
	1217 m	1213 sh	1230	(νC-C + δCH) ald + δCHring
1221 m		1247 sh	1256/1263	δNH(Py+Hyd) + δCH(INH)
1192 vw				νN-N + δCH + νCX
	1184 sh		1181/ 1197	δCH + ρCH_3
	1163 m-w			$\rho_{r}CH_3$

1142 m		1148 w	1166	νN-N + δCH
1098 sh		1106 vw		δCH + νring + νCN
		1096 w	1105	δCH (*o*-HVa + INH)
	1070 s	1078 m	1134	νC-O(OCH_3) + δOH + δNNC + δCH (*o*-HVa)
1062 w		1067 m-w	1067	(δCH + δring) INH
		1030 vw	1091	ν(N-N-C=O)
995 s		1005 m	1011	δring (INH)
	947 s	968 m	1000	δring + νC-O(OCH_3)
	895 w	893 m	962	γCH (*o*-HVa)
888 m-w				γCH + γCX
845 s				γCH + γCX
		853 w	905	δN-C=O
	838 m	839 m	612	γOH
	779 w	780 m	842	δring (*o*-HVa)
	763 s			γCH (ring + ald) *o*-HVa
				(γCH ip + τ ring + γCO) INH
746 m		751 m	790	(γCH ip + γNH + γCO) INH
	737 m	731 s	775	γCH (*o*-HVa)ip
			747	δring (*o*-HVa)
	717 s			δring + δCH *o*-HVa + δ(Ar-O-CH_3)
675 s				δring + νCX + δN-C=O
660 m		686 w	692	(δring + δCH) INH
	642 m			δring (*o*-HVa)
		631 sh/ 608 m,b	675	γ C-C(O)-N + γring (INH)
		568 w		(δC-N-N + δCH C8) *o*-HVa
	534 m-w			δCH(ring + C8)
504 w				τHNNH + γNH + δNCC + δCX + δOCC
		484 vw		
		453 vw	443	γNH (hyd)

X: (CO-NH-N-); hyd: hydrazone; vs: very strong; s: strong; m: medium; w: weak; vw: very weak; b: broad; sh: shoulder; ip: in-phase; op: out-of-phase.

Table S3b. Complete assignment of the IR spectrum of INHVa (**1**). Experimental and calculated frequencies. Data of INH and Va are included for comparison.

INH	Va	INHVa	Calculated	Asignment
		3506 sh		$\nu_{as}H_2O$
	3178 s,b	3420 m,b		$\nu_{s}H_2O$
		3209 m	3524	νNH (hyd)
3304 m		3156 w	3235	νCH (Va)ip
3111 vs				νNH_2
		3080 m	3181	$\nu_{as}CH_3$
3050 w		3046 m	3255/3239	νCH (INH)ip
			3223/3214	νCH(Va)op
3013 w			3195/3191	νCH(INH)op
	3018 w	3020 sh	3843	νOH
	2975 vw	2970 vw	3116	$\nu_{as}CH_3$
	2945 vw	2921 vw	3070	νCH (C8)
	2917 vw		3049	$\nu_{s}CH_3$
	2858 w	2842 vw		νCH (C8)
1667 vs		1665 vs	1818	νC=O
	1665 vs			νC=O (Va)
1634 s				δNH_2
1602 m		1639 sh	1689/1672	νring (Va + INH)
		1599 s,b	1741	νC=N
1556 s			1677/1642	νring(INH)
	1588 w	1557 sh	1585	(δCH + νring)(Va) + νAr-OH
1492 w			1547	(δCH + νring + νAr-C) INH
			1535	δNH + νN-N + δCH(C8)
	1512 m	1510 s	1504/1521	$\delta_{as}CH_3$
	1465 s,b	1471 w	1498	$\delta_{s}CH_3$ + δNH
	1455 m	1455 sh	1477	νring Va
	1430 s	1398 m	1422	δOH + νring(Va) + νAr-OCH_3
1412 s			1454	(δCH + νring)INH
	1397 w	1386 sh	1393	δCH(C8) + δNH + νAr-C(INH)
	1339 vw	1340 vw	1374	δCH(C8) +νC-N
1334 s			1355	δCH (INH)
1321 sh				$\rho_{r}NH_2$
	1300 m	1287 s	1339	νAr-OH + δCH (Va)
	1266 s	1263 m	1320	νAr-OH + δCH(Va)
	1248 sh	1254 m-w	1294	νAr-OCH_3 + νring(Va) + νAr-OH
1221 m		1217 w	1267	νring INH
			1254	δCH (INH)
	1200 m	1204 w	1244	δCH (Va) + $\rho_{r}CH_3$+ δOH
			1233	(δCH + νring) Va + νN-N + δOH
1192 vw		1172 m-w	1214	$\rho_{r}CH_3$ + νN-N
	1173 m		1195	νN-N + δCH (Va) + νO-CH_3
	1154 m		1185	$\rho_{W}CH_3$
1142 m				νN-N + δCH (INH)

	1124 w	1127 m-w, b	1152	(δCH + νring) Va + νO-CH_3
1098 sh		1106 vw		
1062 w		1068 m	1104	(δCH + νring) INH
		1061 sh		
	1029 s	1028 m	1092	νO-CH_3 +(δCH + νring) (Va)
995 s		1006 w	1022	δring INH
		994 sh		
	958 vw	968 vvw	984	γCH ring (Va) + γC(8)H
			973/	γCH ring (Va) + γC(8)H
			871	γCH(Va)
888 m-w		901 w	1007	(γCH + γring) (INH)
			911	γCH (INH)
	858 s	868 vw	854	(γCH + γring)(Va)
845 s				(γCH + γring) (INH)
		842 w,b	874	δAr- C(H)-NN + δring (Va +
			845	INH)
			824	δring (Va) + δC-OH + δC-OCH_3
	813 m	816 m	470 /446	γOH
746 m		751 s	782	(γring + γCH) INH + γ Ar-C(O)-N
			732	γCH(INH) + γCO
	734 m-s			δring (Va)
675 s		688 w	679	δring INH+ δX
660 m		648 sh	651	δN-C=O + δNNC(H) + δring
	632 s	625 m		(INH + Va)
	589 m		627	γring (Va)
		568 w	584	δC-C(O)-N + δring (INH + Va)
	556 w		568	δAr-OH + δring (Va)
			512	δring (Va) +δ Ar-O-CH_3
504 w		481 vw	492	γring (INH)
		456 vw	598	γNH (hyd)
			413	γring INH + γ Ar-C(O)-NN
		418 vw	405	γ Ar-C(H)-NN +

X: (CO-NH-N-); hyd: hydrazone; vs: very strong; s: strong; m: medium; w: weak; vw: very weak; b: broad; sh: shoulder; ip: in-phase; op: out-of-phase.

Table S3c. Complete assignment of the IR spectrum of INHBrVa (**2**). Experimental and calculated frequencies. Data of INH and BrVa are included for comparison.

INH	BrVa	INH-BrVa	Calculated	Asignnment
	3307 s,b	3445 m,b		νH_2O
3304 m		3196 w	3525	νNH (hyd)
3111 vs				νNH_2
	3103 w	3148 w	3237	νCH (BrVa)ip
	3073 w	3094 sh	3226	νCH (BrVa)op
		3079 w	3188	ν_{as} CH_3
3050 w		3066 sh	3254/3238	νCH (INH) ip
3013 w			3196/3193	νCH (INH)op
	3018 vw	3037 m	3837	νOH
	3008 w	3005 vw	3120	ν_{as} CH_3
	2942 w	2922 vw	3076	νCH (C8))
			3051	$\nu_s CH_3$
	2850 w	2850 w		νCH (C8)
	1676 vs			νC=O (BrVa)
1667 vs		1676 vs	1819	νC=O
1634 s				δNH_2
		1638 sh	1679	νring (BrVa)
1602 m			1676	νring (INH)
		1598 s,b	1740	νC=N
1556 s		1565 m	1642	νring (INH)
			1657	νring(BrVa) + δOH
			1570	νAr-OH +νring (BrVa)
			1532	δNH
	1502 m	1498 s	1520/ 1505	$\delta_{as} CH_3$
1492 w			1545	(δCH + νring)INH
	1465 m	1461 m-w	1498	δ_sCH3 + δNH
	1426 s	1418 m	1421	δOH + νring (BrVa)
1412 s			1453	(δCH + νring) INH
		1380 w,b	1390	δNH + δCH (C8)
	1354 s	1362 sh	1370	δCH(C8) + νCN + νAr-C(INH)
1334 s		1340 w	1354	(δCH + νring) INH
1321 sh				$\rho_r NH_2$
	1295 vs	1297 s	1344	νAr-OH +δOH + δCH(ring + C8) BrVa
	1275 sh	1264 sh	1295	νAr-OCH_3 +νAr-OH + δCH(BrVa)
		1250 sh	1291	(δring +δCH) (BrVA) + δOH
		1239 sh		
1221 m			1268	νring (INH)
			1253	δCH (INH)
	1192 m	1198 m	1236	νN-N + δCH (BrVa) νAr-C (BrVa)
1192 vw	1170 sh	1188 m	1213	νN-N
			1223	δCH + ρrCH_3
	1158 s	1157 w	1187	$\rho_r CH_3$
			1186	νO-CH_3 + δCH (BrVa) + δOH

1142 m		1135 m-w	1155	δring(INH) + δ NNC(O) + δ Ar-C(O)N +νCN
1098 sh		1100 vw		
1062 w		1066 w	1104	(δring + δCH) (INH)
	1045 s	1044 m-s	1106	ν O-CH_3 +δring (BrVa)
995 s		1004 vw	1022	δring (INH)
	973 w	985 w	1009	δring(BrVa) + δ Ar-O-CH_3
	959 w	966 vw	976	γCH(Ar-CH)
		953 vw		
888 m-w		901 w	1006	(γCH + γring) (INH)
			877	δring (BrVa) + δ Ar-Br + δ Ar-O-CH_3
	854 s	874 vw	862	γ CH (BrVa)
845 s			873	γCH (INH)
	831 m	840 w,b	457	γOH
	795 w	808 vw	843	δring (BrVa) + δ Ar-OH + δX
746 m		750 w	783	(γCH + γring) (INH)
		729 w	733	γCO+ γCH(INH) + γNH
	734 m	714 sh	720	δring (BrVa)
675 s		690 vw	667	δ X + δring (INH)
660 m	679 s	666 sh	621	δ Ar-OH + δ Ar-O-CH_3 + δring (INH)
		646 w,b		
	602 vw	623 vw	630	γring (BrVa) + γ NNC(H)C
		601 vw		
	586 vw	591 vw	576	δring (BrVa) + δ Ar-C=O
	520 vw	518 vw	303	ν C-Br + δ Ar-Br
504 w		486 vw	494	γring (INH) + γX
		475 vw		
		460 vw		
		454 vw	600	γNH (hyd)
		420 w	422	γ ring (INH + γ Ar-C(H)

X: (CO-NH-N-); hyd: hydrazone; vs: very strong; s: strong; m: medium; w: weak; vw: very weak; b: broad; sh: shoulder; ip: in-phase; op: out-of-phase.

Table S3d. Complete assignment of the IR spectrum of INHClSal (**3**). Experimental and calculated frequencies. Data of INH and ClSal are included for comparison.

INH	ClSal	INH-ClSal	Calculated	Assignment
		3377 m,b		$\nu_{as}H_2O$
	3234 m,b	3259 w,b		$\nu_{s}H_2O$
3304 m		3114 w	3534	νNH (hyd)
3111 vs				νNH_2
	3098 vw	3089 w	3242	νCH (ClSal)ip
	3074 vw			
3050 w		3066 w	3266	νCH (INH) ip
3013 w			3245	νCH (INH)op
	3047 vw	3048 w	3673	νOH
		3027 vw	3218	νCH (ClSal)op
	2925 vw	2926 vw	3110	νCH (C8)
	2878 w	2870 vw,b		νCH (C8)
		2517 m,b	3577	νNH (Py)
1667 vs		1674 vs	1840	νC=O
	1663 vs			νC=O (ClSal)
1634 s				δNH_2
1602 m		1615 sh	1707	νring (INH)
		1603 s,b	1729	νC=N
	1612 w		1696	νring (ClSal)
	1570 w			
		1562 sh	1536	νC-N + δNH(hyd)
1556 s				νring (INH)
1492 w			1560	δNH(Py) + (νring + δCH) INH
	1503 sh	1486 m,b	1530	νring (ClSal) + νAr-C (ClSal)
	1470 s	1451 sh	1476	νAr-OH + νring (ClSal)
	1433 w		1422	νring (ClSal) + δNH(hyd) + δOH
1412 s		1410w		(δCH + νring)INH
	1378 m	1363 m,b	1392	νAr-C(O) +νC-N + δNH(hyd)
	1355 sh		1377	νC-N + δCH (C8) + νAr-C(H)
1334 s		1339 sh	1340	(δCH + νring)(INH)
		1317 w	1280	δNH(Py) + νring(INH)
1321 sh				ρ_rNH_2
	1304 m	1301 m	1306	νAr-OH + (δCH + δring) (ClSal)
	1276 vs	1271 m	1267	δCH(ClSal)
	1267 sh			
1221 m			1233	δNH(Py) + δCH (INH)
	1236 vw	1244 m,b		
	1213 m	1231 sh	1220	(νAr-C + νring + δCH) (ClSal)
	1196 sh			
1192 vw		1182 w, b	1198	νN-N
	1171 m	1174 sh	1161	δCH (ClSal)
	1155 m	1158 sh	1149	ν(ring +δCH) (ClSal)
1142 m		1142 vw	1132	νrings + δCH (INH)
	1116 w	1124 vw	1133	ν(ring +δCH) (ClSal)

	1099 sh 1082 w	1090 sh		
1098 sh		1097 w	1090	(δCH + νCN ring) (INH)
1062 w		1068 vw		δring (INH)
		1052 vw		
	1016 vw			δring (ClSal)
995 s		1003 m-w	1032	δring (INH)
		975 w	1024	γCH (INH)
	962 vw	967 w	999	γ CH (C8)
888 m-w			932	γNH(Py) + γCH (INH)
845 s				
	956 sh	945 m	946	δring (ClSal)
	906 s	885 m	901	γCH (ClSal)
	888 m	870 sh	860	
	841sh			
	831 s	836 m-s	597	γOH
	770 s	783 w	825	δ ring ClSal
746 m		746 m	814	γ Ar-C(O)-N + γ ring(INH)
			762	γ ring(INH)
		729 vw	736	γring (ClSal)
	731 m	715 m-w	730	ν C-Cl + δring (ClSal)
	704, s-b			δring (ClSal)
		703 sh	707	γ C-C(O)-NH
675 s		678 m,b	665	δring (ClSal) + ν C-Cl
660 m			656	δring (INH)
			645	δCX
	646 m-s	650 w	599	δring (ClSal)
		569 w	598	δ CC=O +δ NC=O
	543 m	557 vw	574	γCH (ClSal) + γNH (hyd)
504 w				τHNNH + δNCC
		528 vw	499	δCX + δOCC
	495 vw	487 vw	481	γring (ClSal) + γNH (hyd)
	485 sh	477 vw		
		448 vw	579	γNH (hyd)
		424 w	408	γring (INH)

X: (CO-NH-N-); hyd: hydrazone; vs: very strong; s: strong; m: medium; w: weak; vw: very weak; b: broad; sh: shoulder; ip: in-phase; op: out-of-phase.

Table S3e. Complete assignment of the IR spectrum of INHBrSal (**4**). Experimental and calculated frequencies. Data of INH and BrSal are included for comparison.

INH	BrSal	INH-Brsal	Calculated	Assignament
	3457 w,b	3400 m,b		$\nu_{as}H_2O$
	3228 m,b	3256 m,b		$\nu_{s}H_2O$
3304 m		3113 w	3534	νNH(hyd)
3111 vs				νNH_2
		3091 w	3239	νCH (BrSal)ip
3050 w		3064 w	3266/3261	νCH (INH) ip
3013 w			3255/3245	νCH (INH)op
	3042 vw	3044 w	3674	νOH
		3017 vw	3227/3217	νCH (BrSal)op
	2924 vw	2925 vw	3111	νCH (C8)
	2876 w	2865 vw,b		νCH (C8)
		2410 m,b	3578	νNH (Py)
1667 vs		1676 vs	1839	νC=O
	1672 vs			νC=O (BrSal)
1634 s				δNH_2
1602 m		1619 sh	1707	νring (INH)
		1605 vs,b	1728	νC=N
	1653 sh		1692	νring (BrSal)
	1610 w		1640	νring (BrSal)
			1674	δNH(Py) + νring (INH)
1556 s				νring(INH)
	1565 w	1560 sh	1534	δNH (hyd) + νring(BrSal)
1492 w			1560	δNH(Py) + (νring +δCH)(INH)
			1548	δCH (INH) + νAr-C (INH)
		1481 s	1527	(νring +δCH) (BrSal)
	1466 s	1447 sh	1473	δOH + νring (BrSal)
			1420	δOH + δNH(hyd) + νAr-C (BrSal)
1412 s		1410 w	1382	(δCH + νring) INH
	1373 m	1361 m-w	1392	δNHhyd + νAr-C (INH) + νC-N
			1377	δCH(C8) + νC-N
1334 s		1340 vw	1340	(δCH + νring) INH
		1315 w	1281	(δCH + νring) INH
1321 sh				$\rho_r NH_2$
	1305 m	1301 m	1306	νAr-OH + δCH (BrSal)
			1342	
	1280 sh	1270 m	1269	δCH (BrSal)
	1275 vs			
	1258 sh			
1221 m			1233	δCH (INH) +δNH(Py)
	1224 sh	1244 w	1218	(νAr-C + δCH + νring) (BrSal)
	1208 m	1234 sh		
1192 vw		1197 vw	1197	νN-N
	1171 m	1180 m	1164	δCH (BrSal) + νring (BrSal)

	1156 m	1158 w	1151	δAr-C(O)-NN
1142 m		1130 w	1133	δCH (INH)
	1115 w	1122 sh	1119	(νring+δCH) (BrSal)
1098 sh		1097 vw	1091	(νC-Nring + δCH) (INH)
		1082 w		
1062 w		1067 vw		δring (INH)
		1051 vw		
	1016 vvw			δring (BrSal)
995 s		1003 m-w	1032	δring (INH)
888 m-w		975 sh	1024	γCH (INH)
845 s			1010	γCH (INH))
	961 vw	968 m-w	999	γCH (C8)
	956 sh	939 m-w	936	δring (BrSal) + γCH(INH) +
			930	γNH(py)
	892 m	880 w	900	γCH (BrSal)
	886 sh	870 sh	859	γCH (BrSal)
	831 m	834 m-s	599	γOH
	767 m	783 w	824	δring (BrSal) + δ(H)CNN
746 m		745 m-w	814	γCH(INH) +γCCO
			762	γCH(INH) + γNH(py)
	723 sh	729 w	734	(γring +γCH) (BrSal)
	713 sh	713 sh		
	700 s,b	701 w	650	δring (BrSal)
675 s		677 sh	719	δX + δring (INH)
		672 w	707	γC-C(O)-NH
660 m		631 sh	656	δring (INH)
		626 vw	636	ν C-Br + δCX
		574 sh	597	δC-N-N + δring (BrSal)
		559 w		
	539 m	526 vw	567	γCH (BrSal)
		508 s	317	ν C-Br + δring (ClSal)
504 w				τHNNH + γNH + δNCC + δCX + δOCC
	471 vw	486 vw		δring (BrSal)
	451 mw	476 vw	480	γ(BrSal) + δ NNC(H)
		463 vw	456	δCCO(H) (ClSal)
		447 vw	579	γNH (hyd)
		422 w		

X: (CO-NH-N-); hyd: hydrazone; vs: very strong; s: strong; m: medium; w: weak; vw: very weak; b: broad; sh: shoulder; ip: in-phase; op: out-of-phase.

Table S4a. Atomic coordinates (x 10^4) and equivalent isotropic displacement parameters (Å^2 x 10^3) for (E)-N'-(4-hydroxy-3-methoxybenzylidene)isonicotinohydrazide hydrate.

Atom	x	y	z	U(eq)
C(1)	-1413(4)	2993(3)	8003(3)	56(1)
C(2)	-1726(4)	4002(3)	8207(3)	66(1)
C(3)	-3080(4)	4262(3)	8659(3)	65(1)
C(4)	-4110(4)	3517(3)	8932(3)	57(1)
C(5)	-3785(4)	2502(3)	8734(3)	55(1)
C(6)	-2451(4)	2242(3)	8269(3)	57(1)
C(7)	-4639(5)	783(3)	8805(4)	84(1)
C(8)	-11(4)	2674(3)	7523(3)	64(1)
C(9)	3279(4)	3544(3)	6418(3)	58(1)
C(10)	4633(3)	3054(3)	5953(3)	51(1)
C(11)	4787(4)	2017(3)	5769(3)	58(1)
C(12)	6093(4)	1687(3)	5322(3)	62(1)
C(13)	7071(4)	3281(3)	5232(3)	74(1)
C(14)	5799(4)	3699(3)	5673(3)	68(1)
N(1)	942(3)	3330(2)	7207(2)	63(1)
N(2)	2228(3)	2908(2)	6776(2)	61(1)
N(3)	7239(3)	2291(2)	5065(2)	63(1)
O(1)	-5404(3)	3818(2)	9389(2)	73(1)
O(2)	-4864(3)	1824(2)	9032(2)	71(1)
O(3)	3180(3)	4473(2)	6454(2)	81(1)
O(1W)	2050(5)	639(3)	6688(4)	92(1)

Table S4b. Atomic coordinates (x 10^4) and equivalent isotropic displacement parameters ($Å^2$ x 10^3) for (E)-N'-(5-chlorine-2-hydroxybenzaldehyde)isonicotinohydrazide chloride hydrate. U(eq) is defined as one third of the trace of the orthogonalized U^{ij} tensor.

Atom	x	y	z	U(eq)
C(1)	-2643(4)	8696(2)	9193(2)	42(1)
C(2)	-4660(4)	8864(3)	8978(2)	44(1)
C(3)	-5169(5)	9036(2)	8143(2)	49(1)
C(4)	-3760(5)	9026(2)	7520(2)	49(1)
C(5)	-1780(5)	8840(3)	7723(2)	44(1)
C(6)	-1241(5)	8679(2)	8553(2)	46(1)
C(8)	-1958(5)	8583(2)	10056(2)	46(1)
C(9)	-3116(5)	8556(2)	12184(2)	42(1)
C(10)	-1810(4)	8530(2)	12957(2)	39(1)
C(11)	206(5)	8263(2)	12930(2)	44(1)
C(12)	1312(5)	8312(2)	13652(2)	49(1)
C(13)	-1470(5)	8807(3)	14432(2)	49(1)
C(14)	-2644(4)	8771(3)	13727(2)	45(1)
N(1)	-3102(4)	8623(2)	10689(1)	44(1)
N(2)	-2116(4)	8561(2)	11455(2)	45(1)
N(3)	460(4)	8590(2)	14378(2)	47(1)
O(1)	-6145(3)	8878(2)	9550(2)	59(1)
O(1W)	-8056(4)	9034(3)	11191(2)	63(1)
O(3)	-4932(3)	8579(2)	12254(1)	53(1)
Cl(1)	10(1)	8804(1)	6928(1)	59(1)
Cl(2)	3983(1)	8852(1)	15495(1)	55(1)

Table S4c. Atomic coordinates (x 10^4) and equivalent isotropic displacement parameters (Å^2 x 10^3) for (E)-N'-(5-bromide-2-hydroxybenzaldehyde)isonicotinohydrazide chloride hydrate.

Atom	x	y	z	U(eq)
C(1)	12740(5)	1310(2)	811(2)	37(1)
C(2)	14743(5)	1130(2)	1013(2)	38(1)
C(3)	15276(5)	950(3)	1840(2)	43(1)
C(4)	13884(5)	966(3)	2472(2)	41(1)
C(5)	11909(5)	1169(3)	2275(2)	38(1)
C(6)	11352(5)	1339(3)	1457(2)	39(1)
C(8)	12043(5)	1428(2)	-42(2)	39(1)
C(9)	13193(5)	1444(2)	-2166(2)	36(1)
C(10)	11879(4)	1468(2)	-2931(2)	33(1)
C(11)	9881(5)	1741(2)	-2911(2)	37(1)
C(12)	8777(5)	1696(3)	-3630(2)	43(1)
C(13)	11539(5)	1179(3)	-4399(2)	43(1)
C(14)	12709(5)	1212(3)	-3695(2)	38(1)
N(1)	13183(4)	1383(2)	-674(1)	39(1)
N(2)	12182(4)	1444(2)	-1438(2)	40(1)
N(3)	9616(4)	1407(2)	-4347(2)	40(1)
O(1)	16227(4)	1105(2)	437(2)	54(1)
O(1W)	18150(4)	955(3)	-1183(2)	56(1)
O(3)	15001(3)	1418(2)	-2232(1)	45(1)
Br(1)	9984(1)	1209(1)	3148(1)	47(1)
Cl(2)	6089(1)	1168(1)	-5473(1)	48(1)

Table S5a. Anisotropic displacement parameters ($Å^2$ x 10^3) for (E)-N'-(4-hydroxy-3-methoxybenzylidene)isonicotinohydrazide hydrate.

Atom	U^{11}	U^{22}	U^{33}	U^{23}	U^{13}	U^{12}
C(1)	45(2)	65(2)	62(2)	3(2)	21(2)	0(2)
C(2)	48(2)	71(3)	85(3)	7(2)	28(2)	-8(2)
C(3)	58(2)	61(2)	84(3)	6(2)	32(2)	4(2)
C(4)	46(2)	64(2)	67(2)	1(2)	26(2)	-1(2)
C(5)	46(2)	61(2)	62(2)	0(2)	21(2)	-6(2)
C(6)	47(2)	58(2)	70(2)	-2(2)	20(2)	0(2)
C(7)	78(3)	61(3)	125(4)	-12(3)	50(3)	-18(2)
C(8)	49(2)	79(3)	67(2)	3(2)	25(2)	0(2)
C(9)	44(2)	64(2)	70(2)	1(2)	24(2)	2(2)
C(10)	36(2)	62(2)	59(2)	4(2)	17(1)	4(2)
C(11)	42(2)	61(2)	76(2)	-3(2)	23(2)	-4(2)
C(12)	51(2)	62(2)	78(2)	-2(2)	23(2)	6(2)
C(13)	52(2)	69(3)	109(3)	-12(2)	43(2)	-10(2)
C(14)	57(2)	61(2)	95(3)	-5(2)	40(2)	-3(2)
N(1)	43(2)	79(2)	72(2)	4(2)	28(1)	4(2)
N(2)	45(2)	67(2)	77(2)	3(2)	30(1)	3(2)
N(3)	46(2)	68(2)	80(2)	-6(2)	28(1)	1(2)
O(1)	58(2)	64(2)	107(2)	-2(2)	47(2)	0(1)
O(2)	61(2)	58(2)	106(2)	-5(2)	44(1)	-7(1)
O(3)	65(2)	62(2)	128(3)	3(2)	53(2)	5(1)
O(1W)	90(2)	83(2)	107(3)	8(2)	28(2)	-26(2)

Table S5b. Anisotropic displacement parameters ($Å^2$ x 10^3) for (E)-N'-(5-chlorine-2-hydroxybenzaldehyde)isonicotinohydrazide chloride hydrate. The anisotropic displacement factor exponent takes the form: $-2\pi^2[h^2a^{*2}U^{11}+...+2 h k a^*b^*U^{12}]$.

Atom	U^{11}	U^{22}	U^{33}	U^{23}	U^{13}	U^{12}
C(1)	47(1)	48(2)	32(1)	-2(1)	-6(1)	1(1)
C(2)	45(1)	50(2)	37(1)	-3(1)	-3(1)	-2(1)
C(3)	45(2)	62(2)	40(2)	-2(1)	-13(1)	-2(2)
C(4)	57(2)	54(2)	34(1)	0(1)	-9(1)	-5(1)
C(5)	51(2)	51(2)	30(1)	-2(1)	-1(1)	-1(2)
C(6)	44(1)	54(2)	40(2)	-2(1)	-5(1)	4(1)
C(8)	45(1)	58(2)	35(1)	2(1)	-6(1)	0(2)
C(9)	45(1)	47(2)	33(1)	3(1)	-3(1)	-1(1)
C(10)	39(1)	43(1)	34(1)	4(1)	0(1)	-3(1)
C(11)	44(2)	53(2)	35(1)	3(1)	0(1)	5(1)
C(12)	39(1)	62(2)	45(2)	6(2)	-6(1)	4(1)
C(13)	50(2)	59(2)	37(1)	-2(2)	-1(1)	0(2)
C(14)	39(1)	55(2)	39(1)	2(1)	2(1)	-2(1)
N(1)	44(1)	56(1)	31(1)	1(1)	-9(1)	-2(1)
N(2)	37(1)	65(2)	34(1)	1(1)	-6(1)	0(1)
N(3)	49(1)	57(2)	36(1)	3(1)	-10(1)	-3(1)
O(1)	44(1)	88(2)	45(1)	2(1)	2(1)	1(1)
O(1W)	44(1)	87(2)	57(2)	18(1)	-13(1)	-7(1)
O(3)	38(1)	78(2)	43(1)	8(1)	-7(1)	-2(1)
Cl(1)	61(1)	78(1)	38(1)	-1(1)	7(1)	-4(1)
Cl(2)	48(1)	77(1)	40(1)	-7(1)	-11(1)	9(1)

Table S5c. Anisotropic displacement parameters ($Å^2$ x 10^3) for (E)-N'-(5-bromine-2-hydroxybenzaldehyde)isonicotinohydrazide chloride hydrate.

Atom	U^{11}	U^{22}	U^{33}	U^{23}	U^{13}	U^{12}
C(1)	42(2)	41(2)	27(1)	-2(1)	-3(1)	-2(2)
C(2)	38(1)	44(2)	32(1)	-2(1)	-1(1)	-2(2)
C(3)	35(2)	57(2)	36(2)	-3(1)	-7(1)	1(2)
C(4)	47(2)	50(2)	26(2)	0(1)	-11(1)	-3(2)
C(5)	46(2)	44(2)	24(1)	-2(1)	3(1)	-3(2)
C(6)	34(1)	48(2)	36(2)	0(2)	-5(1)	1(2)
C(8)	38(2)	50(2)	31(2)	2(1)	-6(1)	3(2)
C(9)	41(2)	39(2)	27(1)	4(1)	-4(1)	0(1)
C(10)	35(1)	37(2)	27(1)	3(1)	-4(1)	-3(1)
C(11)	40(2)	43(2)	29(1)	4(1)	0(1)	4(2)
C(12)	39(2)	51(2)	38(2)	5(2)	-6(1)	5(2)
C(13)	46(2)	52(2)	31(2)	-4(2)	-1(1)	-2(2)
C(14)	33(1)	50(2)	32(1)	0(2)	3(1)	-2(2)
N(1)	40(1)	52(2)	26(1)	3(1)	-6(1)	-2(1)
N(2)	35(1)	60(2)	25(1)	0(1)	-8(1)	1(1)
N(3)	41(1)	51(2)	29(1)	0(1)	-11(1)	-4(1)
O(1)	41(1)	85(2)	38(1)	0(2)	4(1)	2(2)
O(1W)	39(1)	78(2)	51(2)	19(2)	-12(1)	-9(1)
O(3)	34(1)	68(1)	34(1)	7(1)	-5(1)	1(1)
Br(1)	50(1)	61(1)	29(1)	0(1)	4(1)	-3(1)
Cl(2)	42(1)	70(1)	33(1)	-6(1)	-8(1)	9(1)

Table S6a. Hydrogen coordinates (x 10^4) and isotropic displacement parameters (Å^2 x 10^3) for (E)-N'-(4-hydroxy-3-methoxybenzylidene)isonicotinohydrazide hydrate.

Atom	x	y	z	U(eq)
H(2)	-1030	4510	8041	79
H(3)	-3296	4945	8778	78
H(6)	-2250	1560	8134	68
H(7A)	-4664	698	8051	126
H(7B)	-5487	386	9031	126
H(7C)	-3613	559	9178	126
H(8)	190	1982	7447	76
H(11)	4026	1556	5944	70
H(12)	6175	992	5191	75
H(13)	7848	3722	5042	88
H(14)	5736	4399	5778	82
H(2A)	2343	2257	6741	73
H(1)	-6020(50)	3230(30)	9570(30)	116(17)
H(1W)	2090(70)	230(40)	7220(30)	180(30)
H(2W)	1460(60)	340(40)	6170(30)	180(30)

Table S6b. Hydrogen coordinates (x 10^4) and isotropic displacement parameters (Å^2 x 10^3) for (E)-N'-(5-chlorine-2-hydroxybenzaldehyde)isonicotinohydrazide chloride hydrate.

Atom	x	y	z	U(eq)
H(3)	-6493	9161	8004	58
H(4)	-4126	9143	6965	58
H(6)	89	8557	8683	55
H(7)	-605	8475	10147	55
H(11)	785	8055	12429	53
H(12)	2660	8153	13640	58
H(13)	-2021	8984	14947	58
H(14)	-4000	8908	13766	53
H(2)	-836	8524	11461	54
H(3N)	1186	8628	14823	56
H(1)	-5630(60)	8800(30)	10020(30)	72(13)
H(1W)	-7980(100)	9570(40)	11030(40)	110(20)
H(2W)	-7230(70)	9000(30)	11490(30)	61(13)

Table S6c. Hydrogen coordinates (x 10^4) and isotropic displacement parameters (Å^2 x 10^3) for (E)-N'-(5-bromine-2-hydroxybenzaldehyde)isonicotinohydrazide chloride hydrate.

Atom	x	y	z	U(eq)
H(3)	16602	815	1968	51
H(4)	14259	843	3022	49
H(6)	10024	1476	1336	47
H(7)	10691	1542	-130	47
H(11)	9301	1951	-2413	45
H(12)	7434	1868	-3619	51
H(13)	12089	997	-4911	51
H(14)	14061	1064	-3731	46
H(2)	10901	1482	-1444	48
H(3N)	8889	1368	-4789	48
H(1)	15770(70)	1280(30)	20(30)	65(15)
H(1W)	18150(90)	400(40)	-1010(30)	90(20)
H(2W)	17200(70)	1000(30)	-1480(30)	60(13)

Table S7a. Potential energy distribution for INHVa (**1**) STR, BEND and TORS indicate internal coordinates associated to bond lengths, bond angles and torsion angles, respectively. Atom numbering is shown in Figure S3.

405	22% TORS 12 11 10 9 + 25% TORS 14 13 12 11 + 28% TORS 17 16 15 14 + 26% TORS 26 15 14 13
413	31% TORS 5 4 3 2 + 17% TORS 6 5 4 3 + 11% BEND 8 7 6 + 6% TORS 8 7 6 5 + 6% BEND 9 7 6 + 5% BEND 12 11 10 + 7% BEND 13 12 10 + 6% BEND 16 15 14 + 6% BEND 19 18 14
446	11% TORS 15 14 13 12 + 11% TORS 17 16 15 14 + 12% TORS 26 15 14 13 + 60% TORS 33 26 15 14
470	28% TORS 15 14 13 12 + 13% TORS 17 16 15 14 + 43% TORS 33 26 15 14
492	7% BEND 4 3 2 + 51% TORS 5 4 3 2 + 8% TORS 8 7 6 5 + 6% BEND 10 9 7 + 7% BEND 12 11 10
512	5% BEND 8 7 6 + 14% BEND 15 14 13 + 27% BEND 16 15 14 + 6% BEND 18 14 13 + 20% BEND 19 18 14 + 5% STR 26 15
568	27% BEND 15 14 13 + 10% STR 16 15 + 9% STR 18 14 + 29% BEND 26 15 14
584	5% BEND 4 3 2 + 5% BEND 6 5 4 + 14% BEND 8 7 6 + 5% BEND 9 7 6 + 5% STR 10 9 + 13% BEND 14 13 12 + 10% BEND 17 16 15 + 18% BEND 18 14 13 + 5% BEND 19 18 14
598	77% TORS 24 9 7 6
627	6% TORS 12 11 10 9 + 13% TORS 14 13 12 11 + 57% TORS 16 15 14 13 + 23% TORS 18 14 13 12 + 9% TORS 28 17 16 15
651	10% BEND 6 5 4 + 20% BEND 8 7 6 + 8% BEND 11 10 9 + 20% BEND 16 15 14
679	21% BEND 3 2 1 + 31% BEND 5 4 3 + 11% BEND 9 7 6 + 6% BEND 10 9 7 + 8% BEND 12 11 10
687	7% BEND 3 2 1 + 12% BEND 4 3 2 + 40% BEND 5 4 3 + 7% BEND 9 7 6 + 10% BEND 10 9 7 +

	8% BEND 12 11 10
722	102% TORS 15 14 13 12 + 62% TORS 17 16 15 14 + 8% TORS 27 16 15 14
732	25% TORS 4 3 2 1 + 25% TORS 6 5 4 3 + 29% TORS 8 7 6 5 + 16% TORS 9 7 6 5 + 6% TORS 21 2 1 6 + 8% TORS 22 4 3 2
759	73% BEND 4 3 2 + 17% STR 7 6 + 7% STR 9 7 + 17% BEND 16 15 14
782	43% TORS 4 3 2 1 + 31% TORS 6 5 4 3 + 22% TORS 9 7 6 5 + 20% TORS 20 1 6 5 + 22% TORS 23 5 4 3
824	6% BEND 4 3 2 + 15% STR 14 13 + 25% STR 15 14 + 12% BEND 15 14 13 + 10% STR 16 15 + 9% STR 18 14 + 13% STR 26 15
845	20% BEND 4 3 2 + 13% BEND 11 10 9 + 14% BEND 12 11 10 + 32% BEND 14 13 12 + 8% BEND 16 15 14 + 7% BEND 17 16 15 + 8% STR 26 15
854	36% TORS 16 15 14 13 + 42% TORS 27 16 15 14 + 32% TORS 28 17 16 15 + 7% TORS 32 13 12 11
871	6% TORS 14 13 12 11 + 80% TORS 32 13 12 11
874	5% TORS 5 4 3 2 + 10% TORS 6 5 4 3 + 8% TORS 7 6 5 4 + 16% TORS 9 7 6 5 + 17% TORS 21 2 1 6 + 16% TORS 22 4 3 2 + 17% TORS 23 5 4 3
912	39% TORS 20 1 6 5 + 20% TORS 21 2 1 6 + 9% TORS 22 4 3 2 + 31% TORS 23 5 4 3
973	7% BEND 16 15 14 + 9% TORS 17 16 15 14 + 25% TORS 25 11 10 9 + 22% TORS 27 16 15 14 + 24% TORS 28 17 16 15
974	11% STR 12 11 + 33% BEND 16 15 14 + 6% BEND 17 16 15 + 8% STR 18 14 + 5% STR 19 18 + 8% TORS 25 11 10 9 + 6% BEND 27 16 15
984	59% TORS 25 11 10 9 + 10% TORS 27 16 15 14 + 20% TORS 28 17 16 15
1007	21% TORS 4 3 2 1 + 30% TORS 6 5 4 3 + 15% TORS 20 1 6 5 + 15% TORS 21 2 1 6 + 24% TORS 22 4 3 2 + 17% TORS 23 5 4 3
1022	8% STR 2 1 + 15% STR 3 2 + 41% BEND 3 2 1 + 14% STR 4 3 + 35% BEND 5 4 3 + 6% BEND 6 5 4 + 6% TORS 22 4 3 2
1027	9% BEND 3 2 1 + 16% TORS 4 3 2 1 + 8% BEND 5 4 3 + 19% TORS 5 4 3 2 + 13% TORS 20 1 6 5 + 26% TORS 21 2 1 6 + 24% TORS 22 4 3 2
1092	31% BEND 15 14 13 + 26% BEND 17 16 15 + 46% STR 19 18 + 6% BEND 32 13 12
1104	14% STR 2 1 + 13% STR 3 2 + 16% BEND 3 2 1 + 6% STR 4 3 + 20% BEND 5 4 3 + 27% BEND 20 1 6 + 5% BEND 23 5 4
1120	18% STR 2 1 + 29% STR 5 4 + 8% BEND 5 4 3 + 10% BEND 20 1 6 + 8% BEND 21 2 1 + 24% BEND 23 5 4
1151	14% STR 17 16 + 16% BEND 17 16 15 + 9% STR 19 18 + 23% BEND 27 16 15 + 33% BEND 28 17 16
1155	32% BEND 4 3 2 + 10% STR 5 4 + 6% STR 6 5 + 19% BEND 6 5 4 + 8% STR 7 6 + 9% STR 9 7 + 10% STR 10 9 + 5% BEND 20 1 6 + 6% BEND 23 5 4
1185	8% TORS 29 19 18 14 + 43% BEND 30 19 18 + 35% BEND 31 19 18 + 5% TORS 31 19 18 14
1195	20% STR 10 9 + 7% STR 12 11 + 5% STR 13 12 + 10% STR 19 18 + 14% BEND 32 13 12
1214	18% STR 10 9 + 5% STR 19 18 + 27% BEND 29 19 18 + 6% TORS 30 19 18 14 + 8% BEND 31 19 18
1233	13% STR 10 9 + 11% STR 12 11 + 5% BEND 15 14 13 + 8% STR 16 15 + 26% BEND 32 13 12 + 14% BEND 33 26 15

1244	7% STR 16 15 + 6% STR 18 14 + 7% STR 19 18 + 16% BEND 27 16 15 + 16% BEND 29 19 18 + 14% BEND 33 26 15
1254	9% STR 3 2 + 14% STR 4 3 + 5% STR 5 4 + 8% BEND 20 1 6 + 21% BEND 21 2 1 + 27% BEND 22 4 3 + 10% BEND 23 5 4
1267	14% STR 2 1 + 36% STR 3 2 + 10% STR 4 3 + 9% STR 5 4 + 7% BEND 5 4 3 + 23% STR 6 5
1294	12% STR 13 12 + 8% STR 14 13 + 15% BEND 15 14 13 + 7% BEND 17 16 15 + 16% STR 18 14 + 5% STR 19 18 + 6% BEND 25 11 10 + 12% STR 26 15 + 6% BEND 28 17 16 + 6% BEND 33 26 15
1320	10% STR 13 12 + 6% BEND 14 13 12 + 18% BEND 16 15 14 + 12% STR 26 15 + 16% BEND 27 16 15 + 24% BEND 28 17 16
1339	13% STR 17 16 + 7% BEND 25 11 10 + 20% STR 26 15 + 21% BEND 32 13 12 + 11% BEND 33 26 15
1355	21% BEND 20 1 6 + 16% BEND 21 2 1 + 17% BEND 22 4 3 + 27% BEND 23 5 4
1374	11% STR 7 6 + 5% BEND 8 7 6 + 21% STR 9 7 + 5% STR 17 16 + 6% BEND 21 2 1 + 32% BEND 25 11 10
1393	8% STR 7 6 + 7% BEND 8 7 6 + 10% STR 9 7 + 30% BEND 24 9 7 + 25% BEND 25 11 10
1422	16% STR 14 13 + 11% BEND 14 13 12 + 10% STR 16 15 + 5% BEND 16 15 14 + 8% STR 18 14 + 6% BEND 28 17 16 + 29% BEND 33 26 15
1454	13% STR 2 1 + 5% STR 3 2 + 11% STR 5 4 + 6% BEND 20 1 6 + 18% BEND 21 2 1 + 26% BEND 22 4 3
1477	11% STR 13 12 + 10% STR 14 13 + 6% BEND 15 14 13 + 12% STR 17 16 + 10% BEND 29 19 18 + 6% BEND 30 19 18 + 9% BEND 31 19 18 + 8% BEND 33 26 15
1498	8% STR 13 12 + 8% BEND 24 9 7 + 22% BEND 29 19 18 + 12% BEND 30 19 18 + 22% BEND 31 19 18
1504	47% TORS 29 19 18 14 + 21% BEND 30 19 18 + 6% TORS 30 19 18 14 + 24% TORS 31 19 18 14
1521	10% BEND 29 19 18 + 45% TORS 30 19 18 14 + 11% BEND 31 19 18 + 25% TORS 31 19 18 14
1534	7% STR 9 7 + 5% STR 10 9 + 5% STR 14 13 + 29% BEND 24 9 7 + 9% BEND 25 11 10
1547	16% BEND 4 3 2 + 6% BEND 5 4 3 + 5% STR 7 6 + 7% BEND 20 1 6 + 16% BEND 21 2 1 + 14% BEND 22 4 3 + 10% BEND 23 5 4
1585	6% STR 12 11 + 6% BEND 15 14 13 + 9% STR 16 15 + 19% BEND 16 15 14 + 13% STR 26 15 + 11% BEND 27 16 15 + 11% BEND 32 13 12
1642	6% STR 3 2 + 25% BEND 3 2 1 + 33% STR 4 3 + 40% STR 6 5 + 20% BEND 6 5 4
1672	27% BEND 14 13 12 + 45% STR 15 14 + 18% STR 17 16 + 24% BEND 17 16 15 + 7% BEND 28 17 16
1677	31% STR 2 1 + 6% STR 3 2 + 9% BEND 3 2 1 + 12% STR 4 3 + 10% STR 5 4 + 15% BEND 5 4 3 + 14% BEND 6 5 4 + 7% BEND 20 1 6
1689	19% STR 13 12 + 16% STR 14 13 + 18% STR 16 15 + 7% BEND 16 15 14 + 13% STR 17 16 + 7% BEND 32 13 12
1741	77% STR 11 10 + 7% BEND 25 11 10
1818	82% STR 8 7 + 6% BEND 24 9 7
3049	10% STR 29 19 + 48% STR 30 19 + 42% STR 31 19
3070	100% STR 25 11

3116	48% STR 30 19 + 52% STR 31 19
3181	90% STR 29 19 + 6% STR 31 19
3191	21% STR 21 2 + 78% STR 22 4
3195	76% STR 21 2 + 21% STR 22 4
3214	99% STR 32 13
3223	41% STR 27 16 + 58% STR 28 17
3235	58% STR 27 16 + 41% STR 28 17
3239	97% STR 20 1
3255	98% STR 23 5
3524	100% STR 24 9
3843	100% STR 33 26

Table S7b. Potential energy distribution for INHBrVa (**2**). STR, BEND and TORS indicate internal coordinates associated to bond lengths, bond angles and torsion angles, respectively. Atom numbering is shown in Figure S3

.

354	7% BEND 6 5 4 + 6% STR 7 6 + 6% STR 15 14 + 18% BEND 15 14 13 + 5% BEND 16 15 14 + 8% BEND 19 18 14 + 24% BEND 26 15 14
381	6% BEND 5 4 3 + 17% BEND 6 5 4 + 18% STR 7 6 + 10% BEND 8 7 6 + 6% BEND 15 14 13 + 14% BEND 19 18 14 + 5% BEND 26 15 14
394	38% TORS 4 3 2 1 + 57% TORS 5 4 3 2 + 6% TORS 20 1 2 3 + 6% TORS 23 5 4 3
407	18% TORS 12 11 10 9 + 24% TORS 14 13 12 11 + 5% TORS 15 14 13 12 + 11% TORS 17 16 15 14 + 38% TORS 26 15 14 13
422	35% TORS 5 4 3 2 + 11% TORS 6 5 4 3 + 7% BEND 8 7 6 + 8% TORS 8 7 6 5 + 6% BEND 9 7 6 + 11% BEND 13 12 11 + 10% BEND 19 18 14
457	102% TORS 33 26 15 14
494	8% BEND 4 3 2 + 45% TORS 5 4 3 2 + 10% TORS 8 7 6 5 + 6% BEND 10 9 7 + 6% BEND 12 11 10
519	6% BEND 8 7 6 + 35% BEND 15 14 13 + 11% BEND 16 15 14 + 14% BEND 19 18 14 + 5% BEND 26 15 14
540	45% TORS 15 14 13 12 + 25% TORS 17 16 15 14 + 10% TORS 18 14 13 12 + 5% TORS 26 15 14 13 + 13% TORS 27 16 15 14
576	6% BEND 6 5 4 + 15% BEND 8 7 6 + 14% BEND 14 13 12 + 5% STR 16 15 + 7% BEND 17 16 15 + 7% STR 18 14 + 6% TORS 24 9 7 6 + 13% BEND 26 15 14
600	6% BEND 9 7 6 + 72% TORS 24 9 7 6
621	8% BEND 4 3 2 + 6% BEND 8 7 6 + 6% BEND 9 7 6 + 6% BEND 13 12 11 + 13% BEND 18 14 13 + 5% BEND 19 18 14 + 14% BEND 26 15 14 + 6% BEND 27 16 15
630	8% TORS 12 11 10 9 + 13% TORS 14 13 12 11 + 19% TORS 15 14 13 12 + 46% TORS 16 15 14 13 + 14% TORS 18 14 13 12 + 6% TORS 28 17 16 15
667	7% BEND 3 2 1 + 6% TORS 4 3 2 1 + 9% BEND 6 5 4 + 9% BEND 8 7 6 + 9% BEND 9 7 6 + 14% BEND 10 9 7 + 7% BEND 11 10 9 + 5% TORS 24 9 7 6
684	28% BEND 3 2 1 + 77% BEND 5 4 3
709	40% BEND 4 3 2 + 6% BEND 9 7 6 + 7% BEND 10 9 7 + 16% BEND 12 11 10 +

	8% BEND 14 13 12 + 8% BEND 17 16 15 + 11% BEND 18 14 13 + 5% STR 27 16
720	74% TORS 15 14 13 12 + 56% TORS 17 16 15 14
733	33% TORS 4 3 2 1 + 33% TORS 6 5 4 3 + 30% TORS 8 7 6 5 + 17% TORS 9 7 6 5 + 7% TORS 21 2 3 4 + 8% TORS 22 4 3 2
780	34% BEND 4 3 2 + 17% TORS 4 3 2 1 + 19% TORS 6 5 4 3 + 8% STR 7 6 + 12% TORS 9 7 6 5 + 9% TORS 20 1 2 3 + 9% TORS 23 5 4 3
783	33% BEND 4 3 2 + 22% TORS 4 3 2 1 + 24% TORS 6 5 4 3 + 8% STR 7 6 + 12% TORS 9 7 6 5 + 12% TORS 20 1 2 3 + 12% TORS 23 5 4 3
843	10% BEND 4 3 2 + 7% BEND 11 10 9 + 5% BEND 12 11 10 + 33% BEND 14 13 12 + 9% STR 15 14 + 10% STR 16 15 + 7% BEND 17 16 15 + 17% STR 26 15
862	7% TORS 14 13 12 11 + 90% TORS 32 13 12 11
873	8% TORS 5 4 3 2 + 12% TORS 6 5 4 3 + 8% TORS 7 6 5 4 + 18% TORS 9 7 6 5 + 6% TORS 20 1 2 3 + 11% TORS 21 2 3 4 + 17% TORS 22 4 3 2 + 19% TORS 23 5 4 3
877	12% STR 14 13 + 17% STR 15 14 + 14% BEND 15 14 13 + 12% BEND 16 15 14 + 17% STR 18 14 + 6% STR 19 18 + 17% STR 27 16
909	5% TORS 17 16 15 14 + 22% TORS 20 1 2 3 + 11% TORS 21 2 3 4 + 14% TORS 23 5 4 3 + 38% TORS 28 17 16 15
913	5% TORS 17 16 15 14 + 18% TORS 20 1 2 3 + 8% TORS 21 2 3 4 + 5% TORS 22 4 3 2 + 16% TORS 23 5 4 3 + 41% TORS 28 17 16 15
976	90% TORS 25 11 10 9
1006	12% TORS 4 3 2 1 + 7% TORS 5 4 3 2 + 7% TORS 6 5 4 3 + 14% TORS 20 1 2 3 + 13% TORS 21 2 3 4 + 25% TORS 22 4 3 2 + 16% TORS 23 5 4 3
1009	16% STR 12 11 + 42% BEND 16 15 14 + 8% STR 18 14 + 8% STR 19 18
1022	8% STR 2 1 + 15% STR 3 2 + 40% BEND 3 2 1 + 14% STR 4 3 + 5% STR 5 4 + 36% BEND 5 4 3 + 5% TORS 21 2 3 4
1027	8% BEND 3 2 1 + 10% TORS 4 3 2 1 + 7% BEND 5 4 3 + 6% TORS 5 4 3 2 + 10% TORS 20 1 2 3 + 33% TORS 21 2 3 4 + 24% TORS 22 4 3 2
1104	9% STR 2 1 + 8% STR 3 2 + 31% BEND 3 2 1 + 7% STR 4 3 + 22% BEND 5 4 3 + 17% BEND 20 1 2 + 7% BEND 23 5 4
1106	31% BEND 15 14 13 + 39% BEND 17 16 15 + 37% STR 19 18 + 8% BEND 28 17 16 + 7% BEND 32 13 12
1119	16% STR 2 1 + 24% STR 5 4 + 6% BEND 5 4 3 + 16% BEND 20 1 2 + 7% BEND 21 2 3 + 23% BEND 23 5 4
1155	38% BEND 4 3 2 + 10% STR 5 4 + 18% BEND 6 5 4 + 8% STR 7 6 + 11% STR 9 7 + 8% STR 10 9 + 9% BEND 20 1 2 + 6% BEND 23 5 4
1186	6% STR 10 9 + 7% STR 12 11 + 28% STR 19 18 + 16% BEND 28 17 16 + 6% BEND 33 26 15
1187	42% BEND 29 19 18 + 41% BEND 30 19 18 + 8% TORS 31 19 18 14
1213	32% STR 10 9 + 6% BEND 28 17 16 + 8% BEND 32 13 12 + 6% BEND 33 26 15
1223	6% STR 14 13 + 7% BEND 28 17 16 + 8% BEND 29 19 18 + 8% TORS 29 19 18 14 + 7% BEND 30 19 18 + 8% TORS 30 19 18 14 + 39% BEND 31 19 18 + 10% BEND 32 13 12
1236	19% STR 10 9 + 11% STR 12 11 + 6% BEND 15 14 13 + 6% STR 16 15 + 5% STR 18 14 + 21% BEND 32 13 12 + 8% BEND 33 26 15
1253	12% STR 3 2 + 14% STR 4 3 + 6% STR 5 4 + 10% BEND 20 1 2 + 25% BEND 21 2 3 + 26% BEND 22 4 3 + 10% BEND 23 5 4
1268	14% STR 2 1 + 35% STR 3 2 + 10% STR 4 3 + 10% STR 5 4 + 7% BEND 5 4 3 + 23% STR 6 5
1291	17% STR 13 12 + 7% BEND 15 14 13 + 15% STR 16 15 + 12% STR 17 16 + 10% BEND 28 17 16 + 17% BEND 33 26 15

1295	18% STR 18 14 + 7% STR 19 18 + 19% STR 26 15 + 23% BEND 28 17 16
1344	13% STR 17 16 + 8% BEND 25 11 10 + 21% STR 26 15 + 18% BEND 32 13 12 + 17% BEND 33 26 15
1354	6% STR 6 5 + 17% BEND 20 1 2 + 14% BEND 21 2 3 + 17% BEND 22 4 3 + 27% BEND 23 5 4
1370	11% STR 7 6 + 6% BEND 8 7 6 + 21% STR 9 7 + 7% STR 17 16 + 6% BEND 21 2 3 + 28% BEND 25 11 10
1390	7% STR 7 6 + 6% BEND 8 7 6 + 9% STR 9 7 + 28% BEND 24 9 7 + 28% BEND 25 11 10
1421	8% STR 12 11 + 18% STR 14 13 + 12% BEND 14 13 12 + 7% STR 16 15 + 13% BEND 16 15 14 + 7% STR 18 14 + 26% BEND 33 26 15
1453	14% STR 2 1 + 6% STR 3 2 + 13% STR 5 4 + 23% BEND 21 2 3 + 26% BEND 22 4 3
1472	11% STR 13 12 + 9% STR 14 13 + 7% BEND 15 14 13 + 17% STR 17 16 + 7% BEND 29 19 18 + 7% BEND 30 19 18 + 9% BEND 31 19 18 + 7% BEND 33 26 15
1498	8% STR 13 12 + 8% BEND 24 9 7 + 18% BEND 29 19 18 + 20% BEND 30 19 18 + 23% BEND 31 19 18
1505	9% BEND 29 19 18 + 16% TORS 29 19 18 14 + 7% BEND 30 19 18 + 15% TORS 30 19 18 14 + 3% TORS 31 19 18 14
1520	6% BEND 29 19 18 + 36% TORS 29 19 18 14 + 6% BEND 30 19 18 + 36% TORS 30 19 18 14 + 12% BEND 31 19 18
1532	7% STR 9 7 + 5% STR 10 9 + 5% STR 18 14 + 30% BEND 24 9 7 + 9% BEND 25 11 10
1545	6% STR 3 2 + 15% BEND 4 3 2 + 7% BEND 5 4 3 + 9% BEND 20 1 2 + 16% BEND 21 2 3 + 15% BEND 22 4 3 + 10% BEND 23 5 4
1571	6% STR 12 11 + 6% STR 13 12 + 7% STR 15 14 + 14% STR 16 15 + 13% BEND 16 15 14 + 17% STR 26 15 + 7% BEND 32 13 12
1642	7% STR 3 2 + 25% BEND 3 2 1 + 33% STR 4 3 + 39% STR 6 5 + 20% BEND 6 5 4
1657	6% STR 13 12 + 30% BEND 14 13 12 + 44% STR 15 14 + 15% STR 17 16 + 27% BEND 17 16 15 + 7% BEND 28 17 16 + 5% BEND 33 26 15
1676	34% STR 2 1 + 13% STR 4 3 + 8% STR 5 4 + 15% BEND 5 4 3 + 6% STR 6 5 + 15% BEND 6 5 4 + 5% BEND 20 1 2
1679	19% STR 13 12 + 19% STR 14 13 + 9% BEND 15 14 13 + 16% STR 16 15 + 13% STR 17 16 + 9% BEND 32 13 12
1740	77% STR 11 10 + 6% BEND 25 11 10
1819	83% STR 8 7 + 6% BEND 24 9 7
3051	46% STR 29 19 + 45% STR 30 19 + 9% STR 31 19
3076	100% STR 25 11
3120	50% STR 29 19 + 50% STR 30 19
3188	90% STR 31 19
3193	31% STR 21 2 + 67% STR 22 4
3196	65% STR 21 2 + 31% STR 22 4
3226	99% STR 32 13
3237	99% STR 28 17
3238	96% STR 20 1
3254	98% STR 23 5
3525	100% STR 24 9
3837	100% STR 33 26

Table **S7c**. Potential energy distribution for INHClSal (**3**). STR, BEND and TORS indicate internal coordinates associated to bond lengths, bond angles and torsion angles, respectively. Atom numbering is shown in Figure S3

408	7% TORS 1 6 5 4 + 6% TORS 1 2 3 4 + 16% TORS 3 4 5 6 + 15% TORS 3 2 1 6 + 5% TORS 6 1 2 19 + 7% TORS 6 5 4 20
459	23% BEND 12 13 26 + 19% BEND 14 13 26
481	8% TORS 9 10 11 12 + 8% TORS 11 12 13 14 + 5% TORS 12 13 14 15 + 7% TORS 12 17 16 15 + 6% TORS 13 14 15 16 + 8% TORS 13 12 17 16 + 11% TORS 17 12 13 26
499	7% BEND 9 10 11 + 10% BEND 11 12 17 + 7% BEND 14 13 26
574	7% TORS 6 7 9 22 + 5% TORS 8 7 9 22 + 5% TORS 11 12 13 26 + 7% TORS 12 17 16 15 + 5% TORS 13 14 15 16 + 14% TORS 14 15 16 17 + 6% TORS 15 16 17 25 + 11% TORS 17 16 15 29
579	30% TORS 6 7 9 22 + 22% TORS 8 7 9 22 + 17% TORS 11 10 9 22
598	36% TORS 12 13 26 30 + 36% TORS 14 13 26 30
598	10% BEND 6 7 8 + 18% BEND 8 7 9
645	9% BEND 6 7 9 + 10% BEND 7 9 10
656	13% BEND 1 2 3 + 12% BEND 2 1 6 + 14% BEND 3 4 5 + 11% BEND 4 5 6
665	6% STR 15 16 + 15% STR 16 24 + 5% BEND 12 17 16 + 8% BEND 12 13 14 + 15% BEND 13 14 15 + 6% BEND 14 15 16 + 7% BEND 14 13 26 + 5% BEND 15 14 28
707	8% TORS 5 6 7 8 + 17% TORS 8 7 9 22
730	7% STR 6 7 + 10% STR 16 24 + 7% BEND 2 3 4 + 7% BEND 10 11 12
736	10% TORS 11 12 13 26 + 8% TORS 12 13 14 28 + 8% TORS 12 13 14 15 + 5% TORS 12 13 26 30 + 7% TORS 13 12 17 16 + 10% TORS 14 13 12 17
762	12% TORS 1 2 3 27 + 7% TORS 1 6 5 21 + 8% TORS 3 2 1 18 + 8% TORS 3 4 5 21 + 12% TORS 5 4 3 27 + 8% TORS 5 6 1 18
787	10% STR 6 7 + 6% STR 7 9 + 6% STR 11 12 + 10% STR 12 13 + 5% STR 12 17 + 9% STR 13 26 + 5% BEND 2 3 4
814	9% TORS 1 6 7 8 + 10% TORS 1 2 3 27 + 10% TORS 5 4 3 27 + 8% TORS 5 6 7 9
825	16% STR 12 13 + 11% STR 13 14 + 10% STR 13 26 + 10% BEND 9 10 11 + 6% BEND 15 16 17
860	8% TORS 12 13 14 28 + 16% TORS 13 14 15 29 + 18% TORS 16 15 14 28 + 7% TORS 17 16 15 29 + 14% TORS 24 16 15 29 + 24% TORS 26 13 14 28
893	10% TORS 1 6 5 21 + 8% TORS 2 3 4 20 + 7% TORS 3 2 1 18 + 11% TORS 3 4 5 21 + 9% TORS 4 3 2 19 + 6% TORS 5 6 1 18 + 8% TORS 6 1 2 19 + 8% TORS 6 5 4 20 + 9% TORS 7 6 5 21 + 6% TORS 7 6 1 18 + 6% TORS 19 2 3 27 + 11% TORS 20 4 3 27
901	23% TORS 11 12 17 25 + 18% TORS 13 12 17 25 + 16% TORS 15 16 17 25 + 26% TORS 24 16 17 25
932	8% TORS 3 2 1 18 + 6% TORS 3 4 5 21 + 5% TORS 5 4 3 27 + 9% TORS 7 6 5 21 + 9% TORS 7 6 1 18 + 16% TORS 19 2 3 27 + 9% TORS 20 4 3 27
946	9% STR 11 12 + 10% STR 16 24 + 6% BEND 12 17 16 + 5% BEND 13 14 28 + 13% BEND 14 15 16 + 7% BEND 15 16 17
989	8% TORS 9 10 11 23 + 7% TORS 13 14 15 29 + 9% TORS 17 16 15 29 + 11% TORS 24 16 15 29 + 6% TORS 26 13 14 28 + 35% TORS 28 14 15 29
999	36% TORS 9 10 11 23 + 6% TORS 10 11 12 13 + 14% TORS 13 12 11 23 + 21% TORS 17 12 11 23 + 6% TORS 28 14 15 29
1009	7% TORS 1 6 5 21 + 8% TORS 2 3 4 20 + 7% TORS 6 5 4 20 + 7% TORS 7 6 5 21 + 17% TORS 20 4 3 27 + 40% TORS 20 4 5 21

1024	6% TORS 4 3 2 19 + 7% TORS 5 6 1 18 + 5% TORS 6 1 2 19 + 10% TORS 7 6 1 18 + 41% TORS 18 1 2 19 + 13% TORS 19 2 3 27
1032	5% STR 1 2 + 7% STR 1 6 + 9% STR 2 3 + 9% STR 3 4 + 5% STR 4 5 + 7% STR 5 6 + 6% BEND 1 6 5 + 6% BEND 1 2 3 + 5% BEND 2 1 6 + 8% BEND 2 3 4 + 6% BEND 3 4 5 + 5% BEND 4 5 6
1090	20% STR 2 3 + 18% STR 3 4 + 11% BEND 6 1 18 + 10% BEND 6 5 21
1132	10% STR 1 2 + 8% STR 4 5 + 6% STR 15 16 + 5% BEND 1 2 19 + 7% BEND 2 1 18 + 9% BEND 4 5 21
1133	9% STR 14 15 + 11% STR 15 16 + 10% STR 16 24 + 8% BEND 12 17 25 + 6% BEND 13 14 28 + 9% BEND 15 14 28
1149	6% STR 1 6 + 8% STR 9 10 + 6% STR 14 15 + 9% BEND 14 15 29 + 6% BEND 15 14 28 + 10% BEND 16 15 29
1161	6% STR 1 6 + 6% STR 6 7 + 5% STR 16 17 + 10% BEND 14 15 29 + 12% BEND 16 15 29
1198	47% STR 9 10 + 8% BEND 10 9 22
1220	15% STR 11 12 + 29% STR 13 14 + 10% STR 15 16 + 7% BEND 13 26 30 + 9% BEND 13 14 28
1233	7% STR 1 2 + 5% STR 2 3 + 9% STR 4 5 + 8% BEND 1 2 19 + 8% BEND 2 1 18 + 14% BEND 3 4 20 + 13% BEND 3 2 19 + 8% BEND 4 5 21 + 9% BEND 5 4 20 + 6% BEND 6 1 18 + 5% BEND 6 5 21
1267	13% STR 12 17 + 20% BEND 12 17 25 + 9% BEND 13 14 28 + 6% BEND 15 14 28 + 18% BEND 16 17 25
1280	23% STR 2 3 + 25% STR 3 4 + 5% STR 5 6 + 9% BEND 2 3 27 + 9% BEND 4 3 27
1306	7% STR 11 12 + 10% STR 12 17 + 36% STR 13 26 + 10% BEND 14 15 29
1340	8% STR 1 6 + 10% STR 5 6 + 12% BEND 1 2 19 + 5% BEND 2 1 18 + 10% BEND 3 4 20 + 11% BEND 3 2 19 + 7% BEND 4 5 21 + 12% BEND 5 4 20 + 7% BEND 6 1 18 + 8% BEND 6 5 21
1344	7% STR 11 12 + 12% STR 12 13 + 7% STR 13 26 + 11% STR 14 15 + 6% STR 15 16 + 25% STR 16 17 + 7% BEND 12 11 23 + 6% BEND 15 14 28
1377	15% STR 7 9 + 6% STR 10 11 + 22% BEND 10 11 23 + 12% BEND 12 11 23
1382	13% STR 1 2 + 14% STR 4 5 + 9% BEND 2 3 27 + 8% BEND 4 3 27 + 6% BEND 4 5 21 + 7% BEND 6 1 18 + 9% BEND 6 5 21
1392	5% STR 1 2 + 10% STR 6 7 + 18% STR 7 9 + 17% BEND 7 9 22 + 6% BEND 8 7 9 + 9% BEND 10 9 22
1422	5% STR 11 12 + 9% STR 12 17 + 9% STR 14 15 + 6% BEND 7 9 22 + 33% BEND 13 26 30 + 7% BEND 16 15 29
1476	9% STR 12 17 + 7% STR 15 16 + 10% STR 16 17 + 30% BEND 13 26 30
1530	7% STR 11 12 + 11% STR 12 13 + 7% STR 13 14 + 6% STR 13 26 + 9% STR 15 16 + 7% BEND 12 17 25 + 9% BEND 13 14 28 + 5% BEND 14 15 29 + 8% BEND 15 14 28 + 6% BEND 16 17 25
1536	7% STR 7 9 + 6% STR 16 17 + 9% BEND 7 9 22 + 15% BEND 10 9 22
1548	5% STR 3 4 + 10% STR 5 6 + 6% STR 6 7 + 5% STR 7 9 + 5% BEND 2 1 18 + 7% BEND 3 4 20 +7% BEND 4 5 21 + 9% BEND 5 4 20
1560	7% STR 1 2 + 12% STR 1 6 + 6% STR 4 5 + 10% STR 5 6 + 12% BEND 2 3 27 + 6% BEND 3 4 20 + 8% BEND 3 2 19 + 11% BEND 4 3 27
1645	20% STR 12 13 + 6% STR 12 17 + 16% STR 14 15 + 18% STR 15 16 + 9% BEND 13 26 30
1674	11% STR 1 6 + 16% STR 2 3 + 14% STR 3 4 + 14% STR 5 6 + 13% BEND 2 3 27 + 14% BEND 4 3 27
1696	12% STR 12 17 + 23% STR 13 14 + 10% STR 14 15 + 20% STR 16 17
1707	24% STR 1 2 + 6% STR 1 6 + 7% STR 3 4 + 21% STR 4 5 + 5% BEND 3 2 19

1729	71% STR 10 11
1840	6% STR 7 9 + 83% STR 7 8
3111	100% STR 11 23
3218	99% STR 17 25
3230	53% STR 14 28 + 47% STR 15 29
3242	47% STR 14 28 + 53% STR 15 29
3245	87% STR 1 18 + 13% STR 2 19
3255	70% STR 4 20 + 30% STR 5 21
3260	13% STR 1 18 + 85% STR 2 19
3266	30% STR 4 20 + 68% STR 5 21
3534	100% STR 9 22
3577	100% STR 3 27
3674	100% STR 26 30

Table S7d. Potential energy distribution for INHBrSal (**4**). STR, BEND and TORS indicate internal coordinates associated to bond lengths, bond angles and torsion angles, respectively. Atom numbering is shown in Figure S3

.

317	8% STR 11 12 + 16% STR 16 30 + 6% BEND 6 7 8 + 8% BEND 9 10 11 + 6% BEND 11 12 13 + 7% BEND 13 12 17 + 6% BEND 15 16 17
360	11% TORS 9 10 11 12 + 6% TORS 11 12 17 16 + 9% TORS 13 14 15 16 + 5% TORS 13 12 17 16 + 8% TORS 14 15 16 30 + 14% TORS 15 14 13 18
365	24% STR 6 7 + 9% BEND 1 6 5 + 7% BEND 8 7 9 + 5% BEND 11 12 13
394	6% BEND 6 7 8 + 6% BEND 6 7 9 + 8% BEND 11 12 17 + 8% BEND 12 13 18 + 6% TORS 2 3 4 5 + 8% TORS 2 1 6 5
408	6% TORS 1 6 5 4 + 6% TORS 1 2 3 4 + 16% TORS 3 4 5 6 + 15% TORS 3 2 1 6 + 5% TORS 6 1 2 20 + 7% TORS 6 5 4 21
457	24% BEND 12 13 18 + 24% BEND 14 13 18
480	8% TORS 9 10 11 12 + 8% TORS 11 12 13 14 + 5% TORS 12 13 14 15 + 7% TORS 12 17 16 15 + 6% TORS 13 14 15 16 + 7% TORS 13 12 17 16 + 11% TORS 17 12 13 18
496	7% BEND 9 10 11 + 9% BEND 11 12 17 + 7% BEND 14 13 18
567	6% TORS 11 12 13 18 + 10% TORS 12 17 16 15 + 7% TORS 13 14 15 16 + 18% TORS 14 15 16 17 + 7% TORS 15 16 17 25 + 13% TORS 17 16 15 29
579	36% TORS 6 7 9 23 + 26% TORS 8 7 9 23 + 21% TORS 11 10 9 23
597	14% BEND 6 7 8 + 17% BEND 8 7 9 + 5% BEND 11 12 13
599	39% TORS 12 13 18 26 + 41% TORS 14 13 18 26
636	5% STR 13 18 + 13% STR 16 30 + 7% BEND 6 7 9 + 6% BEND 7 9 10 + 9% BEND 12 13 14 + 5% BEND 13 14 15
650	5% BEND 12 17 16 + 10% BEND 13 14 15
656	10% BEND 1 2 3 + 11% BEND 2 1 6 + 13% BEND 3 4 5 + 8% BEND 4 5 6
707	8% TORS 5 6 7 8 + 17% TORS 8 7 9 23

719	6% STR 6 7 + 6% STR 16 30 + 7% BEND 2 3 4 + 10% BEND 10 11 12 + 5% BEND 11 12 13
734	11% TORS 11 12 13 18 + 9% TORS 12 13 14 28 + 9% TORS 12 13 14 15 + 6% TORS 12 13 18 26 + 5% TORS 13 14 15 16 + 8% TORS 13 12 17 16 + 11% TORS 14 13 12 17 + 5% TORS 16 15 14 28
762	12% TORS 1 2 3 27 + 7% TORS 1 6 5 22 + 8% TORS 3 4 5 22 + 8% TORS 3 2 1 19 + 12% TORS 5 4 3 27 + 7% TORS 5 6 1 19
783	13% STR 6 7 + 7% STR 7 9 + 6% STR 11 12 + 9% STR 12 13 + 6% STR 13 18 + 7% BEND 2 3 4
814	8% TORS 1 6 7 8 + 10% TORS 1 2 3 27 + 10% TORS 5 4 3 27 + 8% TORS 5 6 7 9
824	16% STR 12 13 + 11% STR 13 14 + 12% STR 13 18 + 9% BEND 9 10 11+ 7% BEND 15 16 17
859	8% TORS 12 13 14 28 + 16% TORS 13 14 15 29 + 18% TORS 16 15 14 28 + 7% TORS 17 16 15 29 + 24% TORS 18 13 14 28 + 13% TORS 29 15 16 30
893	10% TORS 1 6 5 22 + 8% TORS 2 3 4 21 + 11% TORS 3 4 5 22 + 7% TORS 3 2 1 19 + 9% TORS 4 3 2 20 + 6% TORS 5 6 1 19 + 8% TORS 6 1 2 20 + 8% TORS 6 5 4 21 + 6% TORS 7 6 1 19 + 9% TORS 7 6 5 22 + 6% TORS 20 2 3 27 + 11% TORS 21 4 3 27
900	23% TORS 11 12 17 25 + 18% TORS 13 12 17 25 + 17% TORS 15 16 17 25 + 25% TORS 25 17 16 30
930	6% BEND 14 15 16 + 9% TORS 20 2 3 27 + 5% TORS 21 4 3 27
936	7% BEND 14 15 16 + 8% TORS 20 2 3 27
988	8% TORS 9 10 11 24 + 7% TORS 13 14 15 29 + 9% TORS 17 16 15 29 + 6% TORS 18 13 14 28 + 35% TORS 28 14 15 29 + 11% TORS 29 15 16 30
999	36% TORS 9 10 11 24 + 6% TORS 10 11 12 13 + 14% TORS 13 12 11 24 + 21% TORS 17 12 11 24 + 6% TORS 28 14 15 29
1010	7% TORS 1 6 5 22 + 7% TORS 2 3 4 21 + 7% TORS 6 5 4 21 + 7% TORS 7 6 5 22 + 40% TORS 21 4 5 22 + 17% TORS 21 4 3 27
1024	6% TORS 4 3 2 20 + 7% TORS 5 6 1 19 + 5% TORS 6 1 2 20 + 10% TORS 7 6 1 19 + 41% TORS 19 1 2 20 + 13% TORS 20 2 3 27
1032	5% STR 1 2 + 7% STR 1 6 + 9% STR 2 3 + 9% STR 3 4 + 5% STR 4 5 + 7% STR 5 6 + 6% BEND 1 2 3 + 6% BEND 1 6 5 + 5% BEND 2 1 6 + 8% BEND 2 3 4 + 6% BEND 3 4 5 + 5% BEND 4 5 6
1091	21% STR 2 3 + 18% STR 3 4 + 11% BEND 6 1 19 + 10% BEND 6 5 22
1119	13% STR 14 15 + 23% STR 15 16 + 10% STR 16 30 + 9% STR 16 17 + 9% BEND 12 17 25 + 9% BEND 13 14 28 + 12% BEND 15 14 28 + 6% BEND 16 17 25
1133	14% STR 1 2 + 7% STR 3 4 + 13% STR 4 5 + 7% BEND 1 2 20 + 12% BEND 2 1 19 + 12% BEND 4 5 22 + 6% BEND 5 4 21
1151	8% STR 1 6 + 6% STR 5 6 + 6% STR 6 7 + 5% STR 7 9 + 10% STR 9 10 + 5% BEND 14 15 29 + 6% BEND 16 15 29
1164	6% STR 14 15 + 7% STR 16 17 + 13% BEND 14 15 29 + 7% BEND 15 14 28 + 15% BEND 16 15 29

1197	46% STR 9 10 + 8% BEND 10 9 23
1218	16% STR 11 12 + 28% STR 13 14 + 9% STR 15 16 + 6% BEND 13 18 26 + 9% BEND 13 14 28
1233	7% STR 1 2 + 5% STR 2 3 + 9% STR 4 5 + 8% BEND 1 2 20 + 8% BEND 2 1 19 + 14% BEND 3 4 21 + 13% BEND 3 2 20 + 8% BEND 4 5 22 + 9% BEND 5 4 21 + 6% BEND 6 1 19 + 5% BEND 6 5 22
1269	13% STR 12 17 + 21% BEND 12 17 25 + 9% BEND 13 14 28 + 5% BEND 15 14 28 + 19% BEND 16 17 25
1281	23% STR 2 3 + 25% STR 3 4 + 5% STR 5 6 + 9% BEND 2 3 27 + 9% BEND 4 3 27
1306	7% STR 11 12 + 10% STR 12 17 + 35% STR 13 18 + 10% BEND 14 15 29 + 5% BEND 16 15 29
1340	8% STR 1 6 +10% STR 5 6 + 12% BEND 1 2 20 + 5% BEND 2 1 19 +10% BEND 3 4 21 + 11% BEND 3 2 20 + 7% BEND 4 5 22 + 12% BEND 5 4 21 + 7% BEND 6 1 19 + 8% BEND 6 5 22
1342	7% STR 11 12 + 11% STR 12 13 + 8% STR 13 18 + 12% STR 14 15 + 7% STR 15 16 + 25% STR 16 17 + 6% BEND 12 11 24 + 6% BEND 15 14 28
1377	14% STR 7 9 + 6% STR 10 11 + 24% BEND 10 11 24 + 13% BEND 12 11 24
1382	13% STR 1 2 + 15% STR 4 5 + 9% BEND 2 3 27 + 8% BEND 4 3 27 + 7% BEND 4 5 22 + 7% BEND 6 1 19 + 10% BEND 6 5 22
1392	5% STR 1 2 + 11% STR 6 7 + 18% STR 7 9 + 16% BEND 7 9 23 + 6% BEND 8 7 9 + 8% BEND 10 9 23
1420	5% STR 11 12 + 9% STR 12 17 + 9% STR 14 15 + 7% BEND 7 9 23 + 31% BEND 13 18 26 + 8% BEND 16 15 29
1473	8% STR 12 17 + 7% STR 15 16 + 10% STR 16 17 + 32% BEND 13 18 26
1527	6% STR 11 12 + 12% STR 12 13 + 8% STR 13 14 + 8% STR 13 18 + 9% STR 15 16 + 8% BEND 12 17 25 + 9% BEND 13 14 28 + 6% BEND 14 15 29 + 9% BEND 15 14 28 + 6% BEND 16 17 25
1534	8% STR 7 9 + 5% STR 16 17 + 10% BEND 7 9 23 + 17% BEND 10 9 23
1548	5% STR 3 4 + 10% STR 5 6 + 6% STR 6 7 + 5% BEND 1 2 20 + 5% BEND 2 1 19 + 7% BEND 3 4 21 + 7% BEND 4 5 22 + 9% BEND 5 4 21
1560	7% STR 1 2 + 12% STR 1 6 + 6% STR 4 5 + 10% STR 5 6 + 12% BEND 2 3 27 + 7% BEND 3 4 21 + 8% BEND 3 2 20 + 12% BEND 4 3 27
1640	20% STR 12 13 + 7% STR 12 17 +17% STR 14 15 + 17% STR 15 16 + 9% BEND 13 18 26
1674	11% STR 1 6 + 16% STR 2 3 + 14% STR 3 4 + 14% STR 5 6 + 13% BEND 2 3 27 + 14% BEND 4 3 27
1692	11% STR 12 17 +24% STR 13 14 + 9% STR 14 15 + 19% STR 16 17 + 6% BEND 13 18 26
1707	24% STR 1 2 + 7% STR 1 6 + 7% STR 3 4 + 21% STR 4 5 + 5% BEND 3 2 20
1728	72% STR 10 11
1839	6% STR 7 9 + 83% STR 7 8
3111	100% STR 11 24

3217	99% STR 17 25
3227	63% STR 14 28 + 37% STR 15 29
3239	37% STR 14 28 + 63% STR 15 29
3245	86% STR 1 19 + 13% STR 2 20
3255	72% STR 4 21 + 27% STR 5 22
3260	13% STR 1 19 + 85% STR 2 20
3266	27% STR 4 21 + 71% STR 5 22
3534	100% STR 9 23
3578	100% STR 3 27
3674	100% STR 18 26

Supplementary Material. Figures

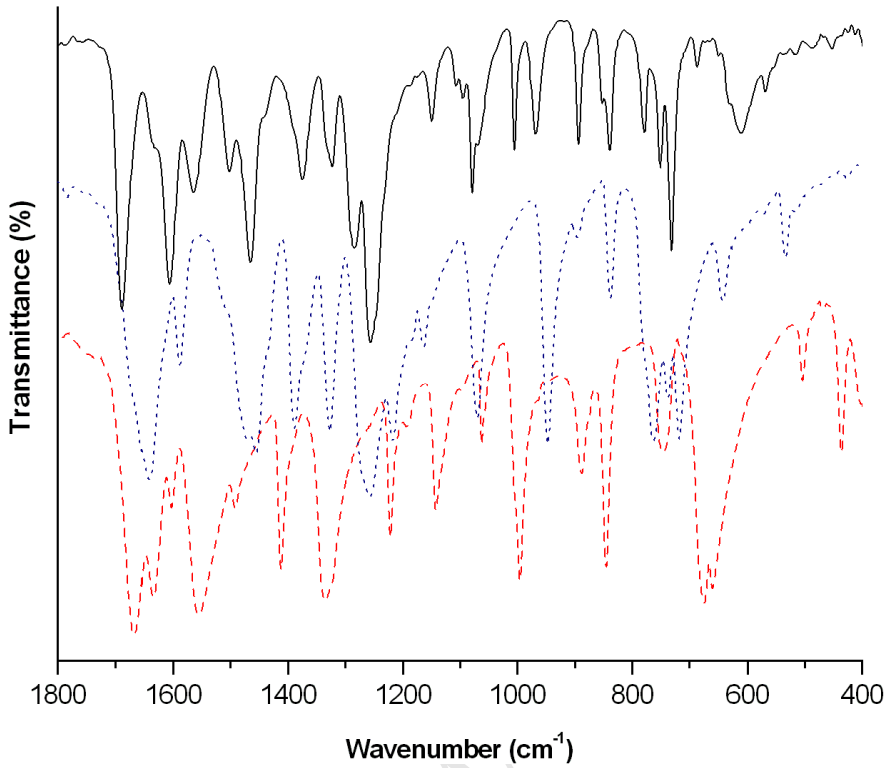

Figure S1a. Experimental IR spectrum of INH (red, dashed), oHVa (blue, dotted) and INHoVa, in the 1800–400 cm^{-1} spectral range.

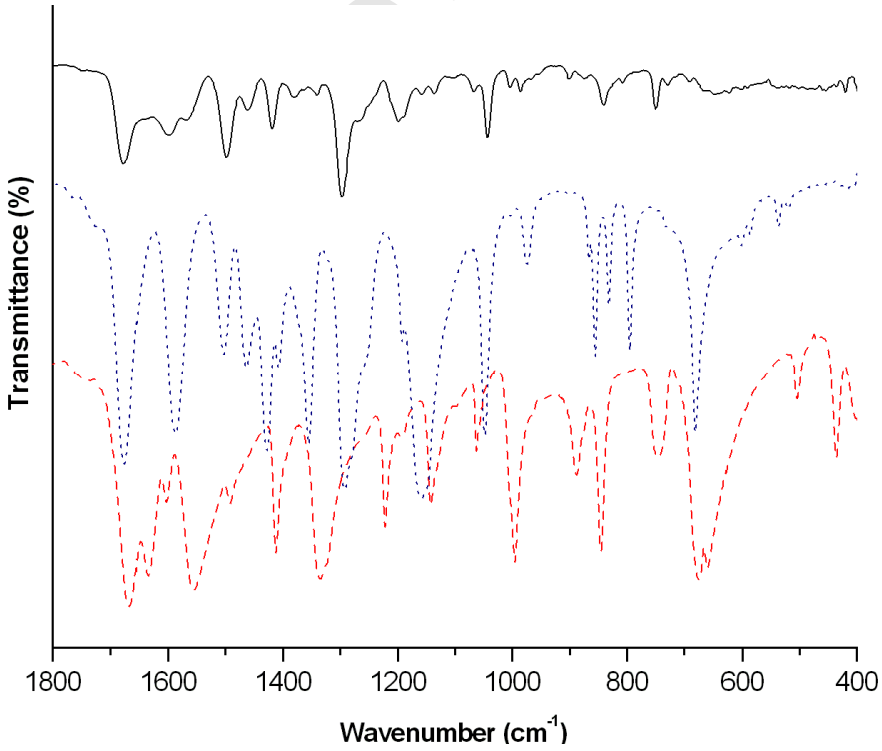

Figure S1b. Experimental IR spectrum of INH (red, dashed), BrVa (blue, dotted) and INHBrVa, in the 1800–400 cm^{-1} spectral range.

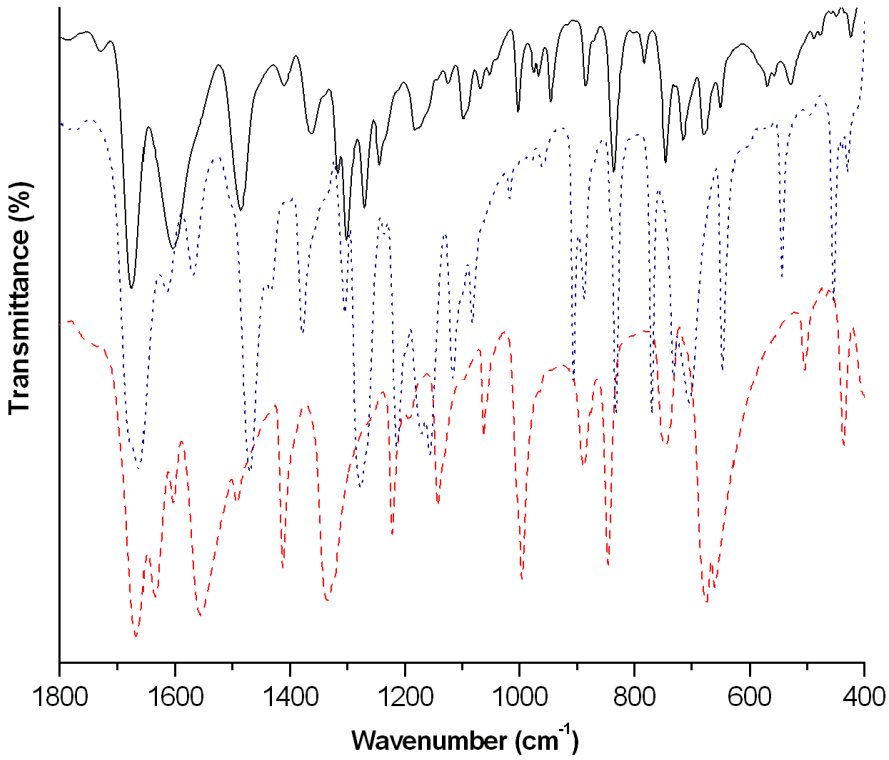

Figure S1c. Experimental IR spectrum of INH (red, dashed), ClSal (blue, dotted) and INHClSal, in the 1800–400 cm^{-1} spectral range.

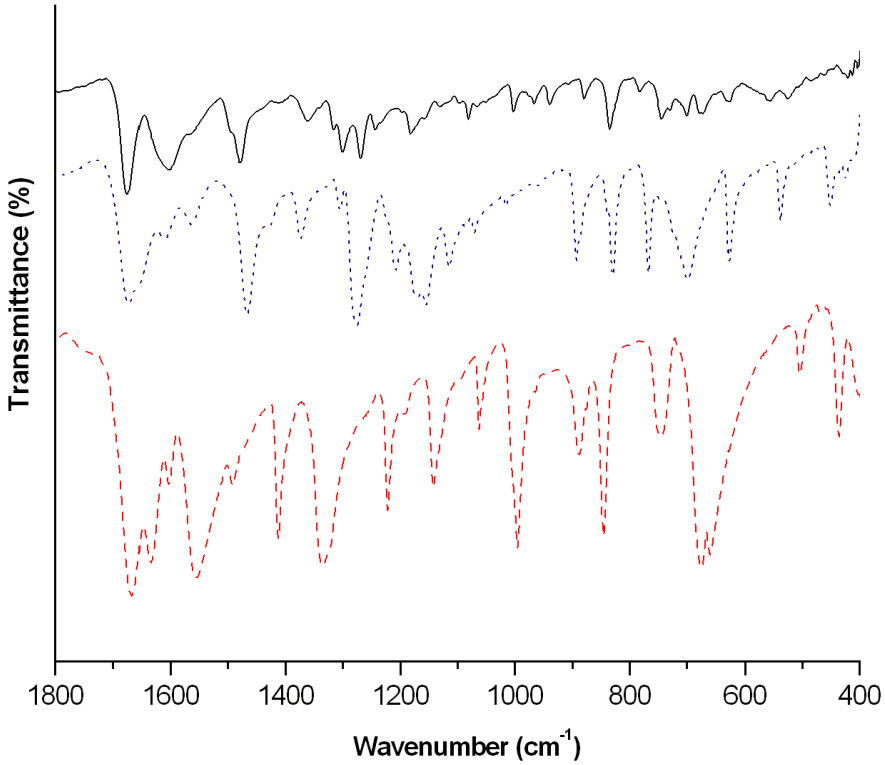

Figure S1d. Experimental IR spectrum of INH (red, dashed), BrSal (blue, dotted) and INHBrSal, in the 1800–400 cm^{-1} spectral range.

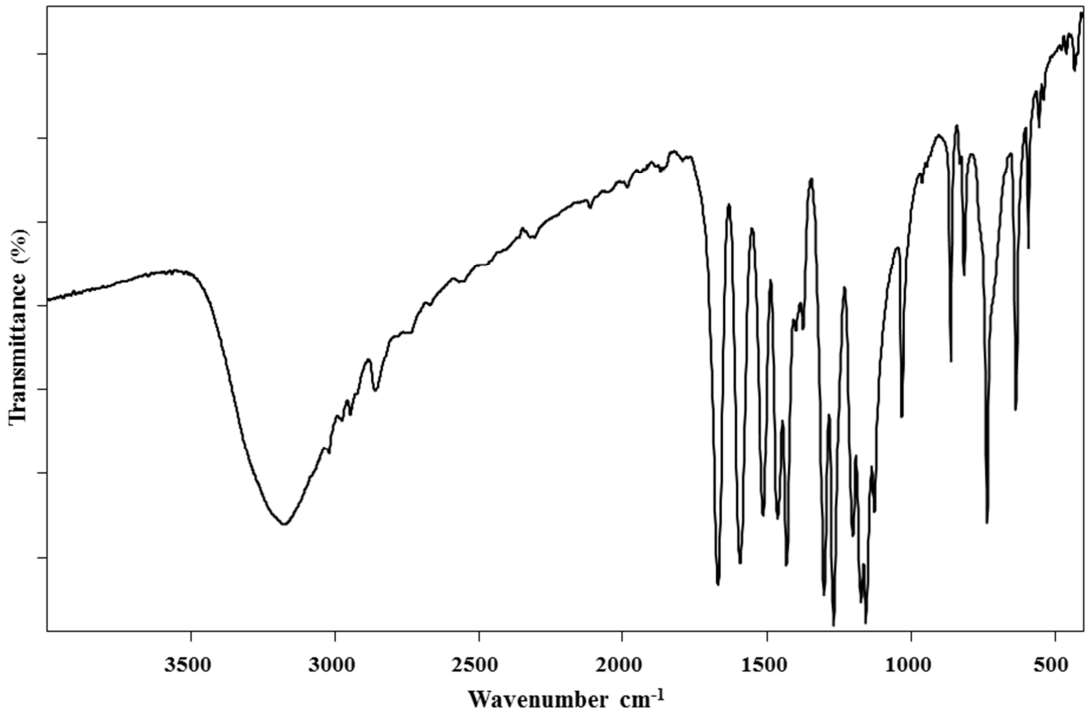

Figure S1e. Experimental IR spectrum of vanillin (Va) in the 4000-400 cm^{-1} spectral range.

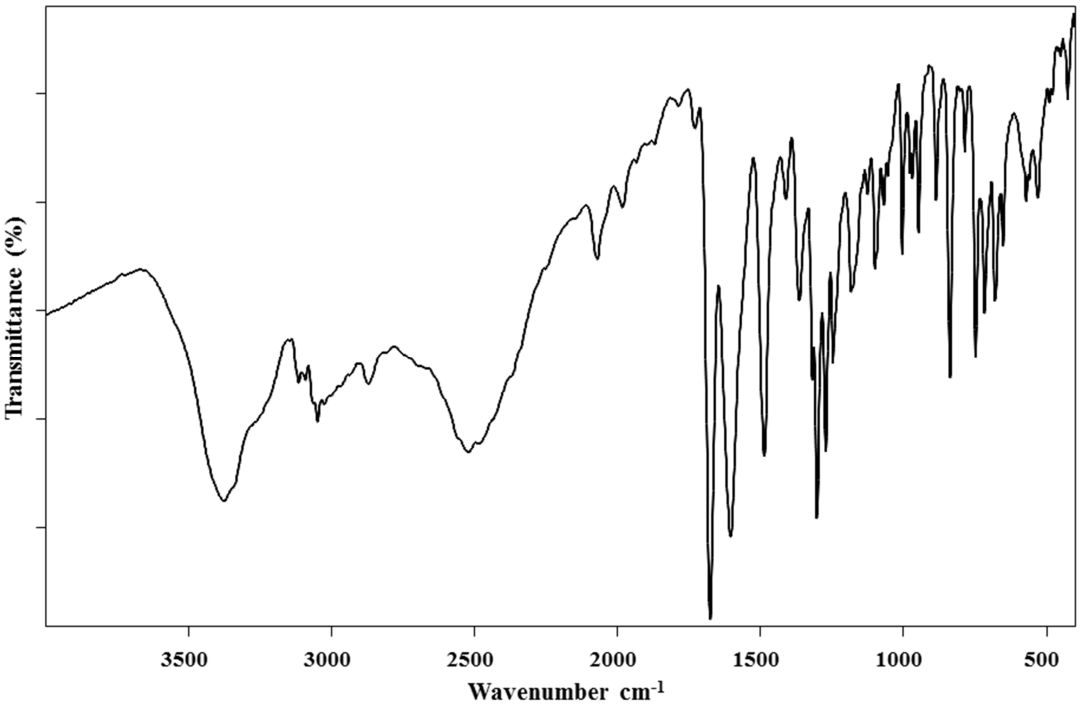

Figure S1f. Experimental IR spectrum of INHClSal (**3**) in the 4000-400 cm^{-1} spectral range

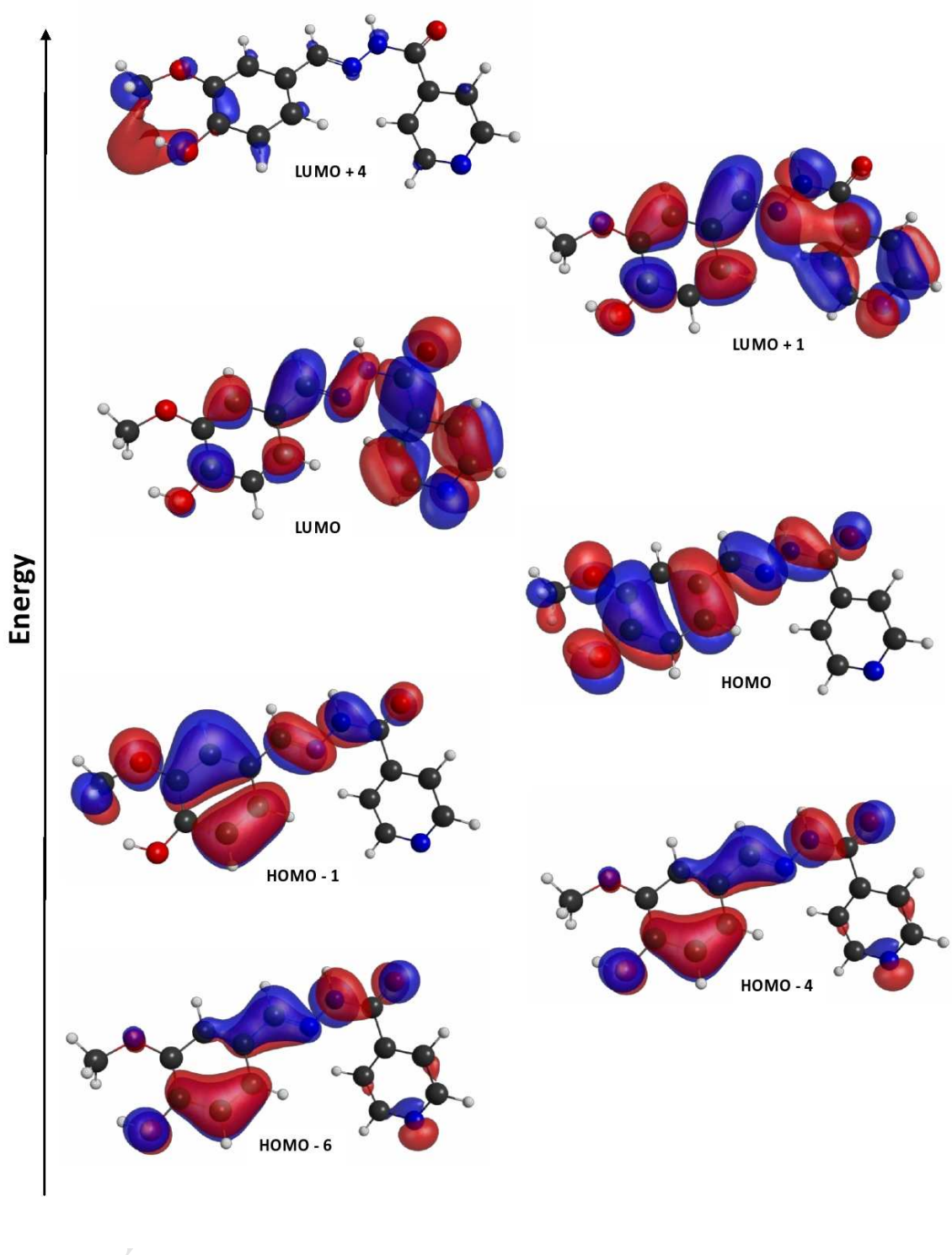

Figure S2a. Energy scale and MOs involved in the electronic transitions for INHVa.

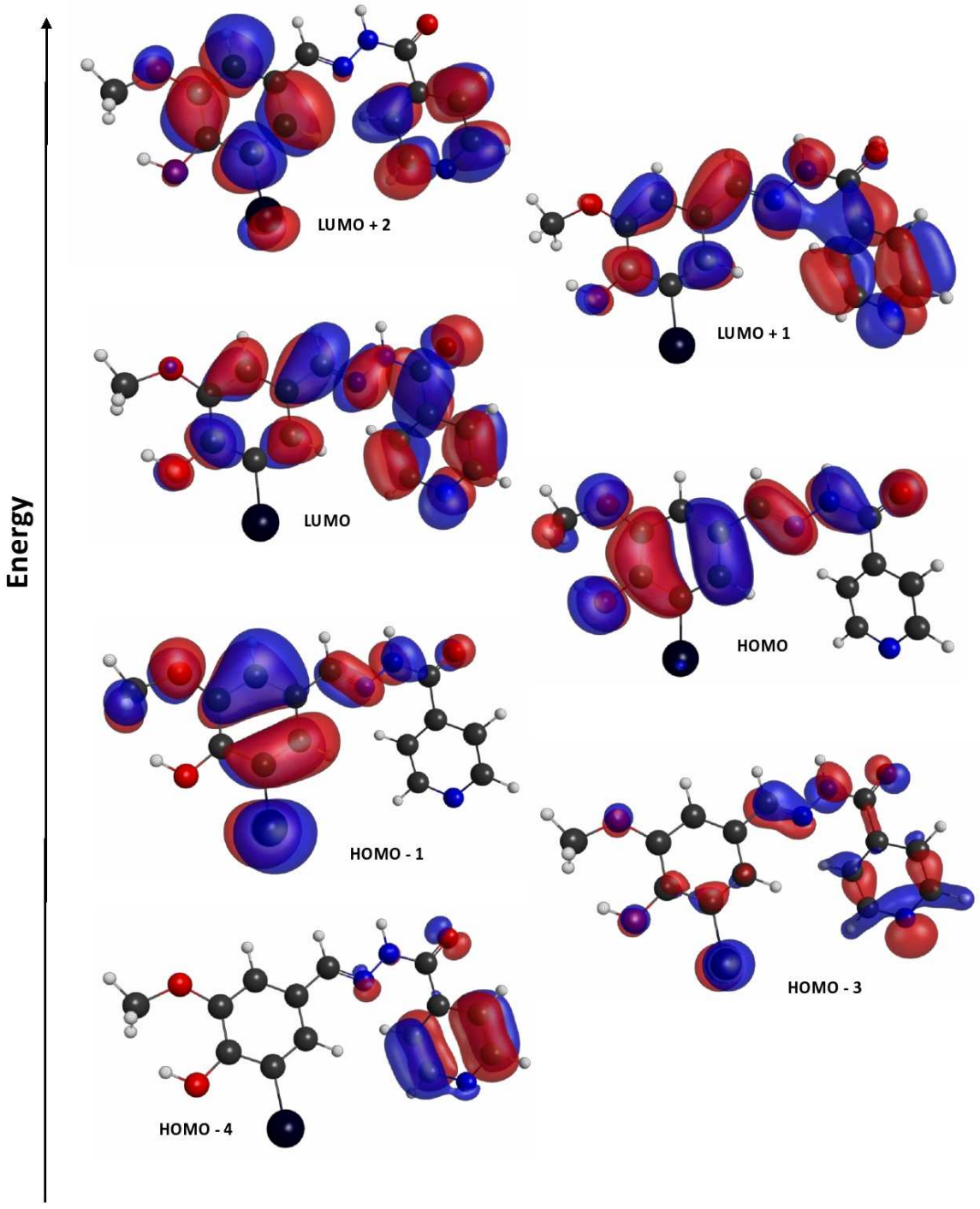

Figure S2b. Energy scale and MOs involved in the electronic transitions for INHBrVa.

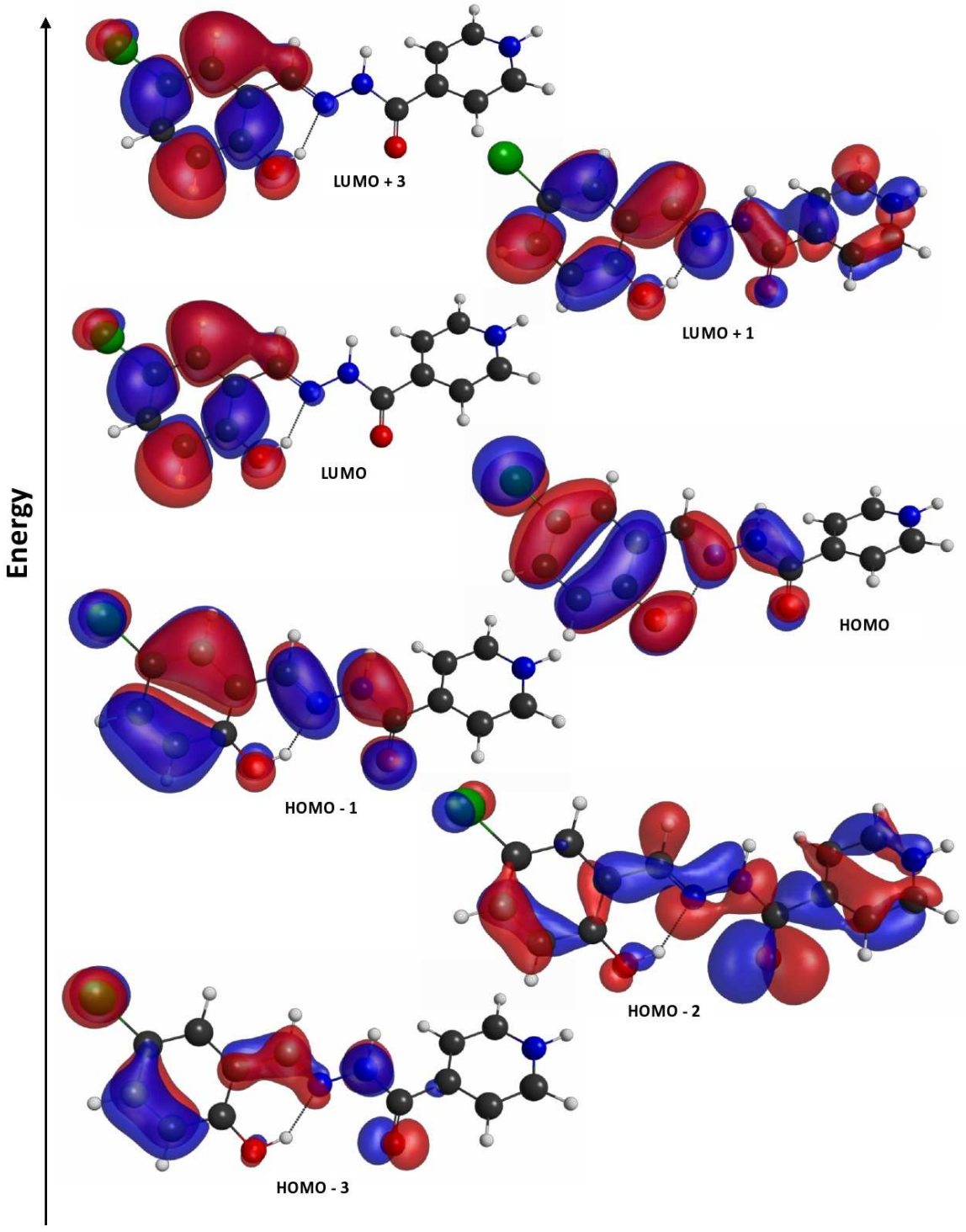

Figure S2c. Energy scale and MOs involved in the electronic transitions for INHClSal.

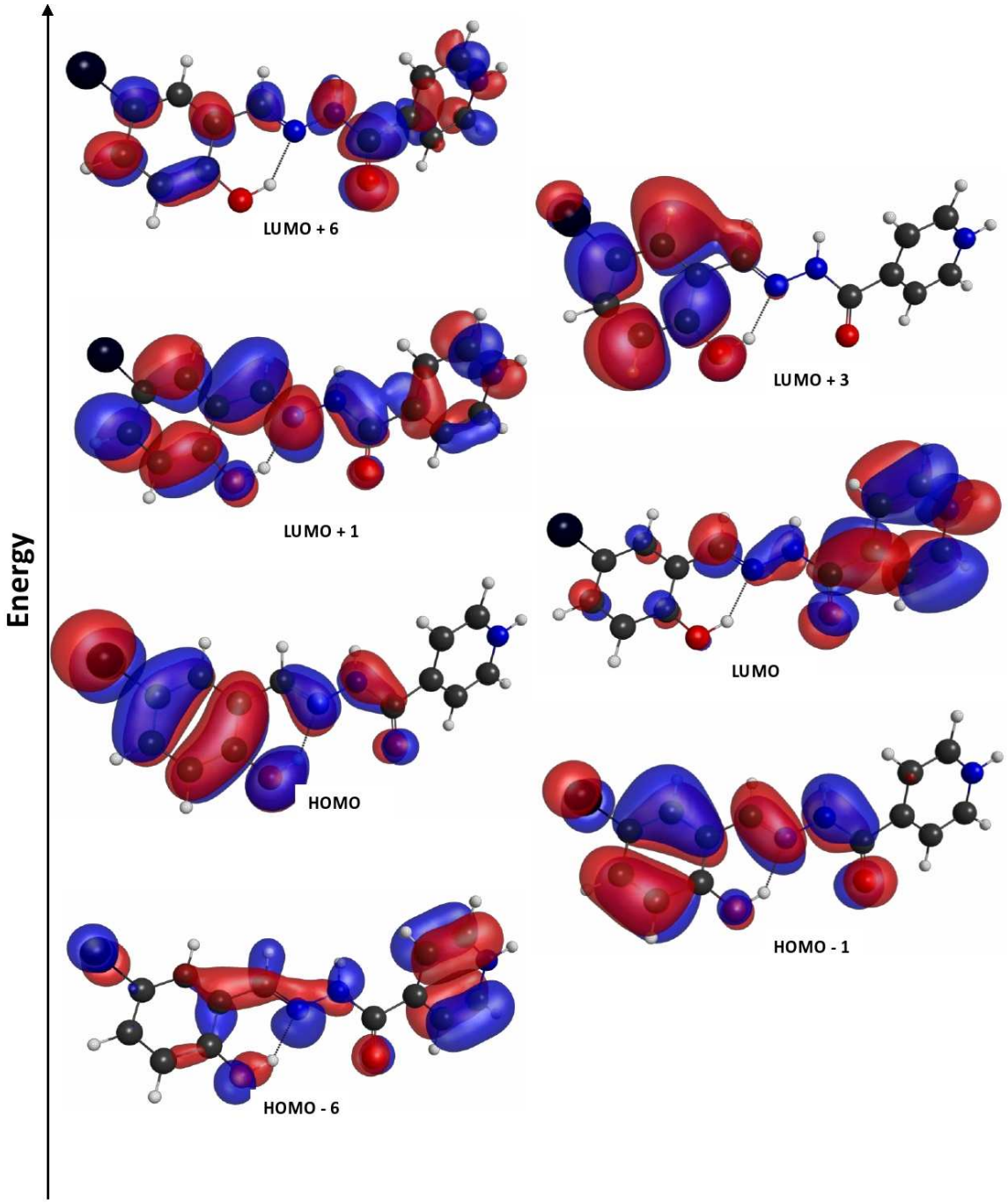

Figure S2d. Energy scale and MOs involved in the electronic transitions for INHBrSal.

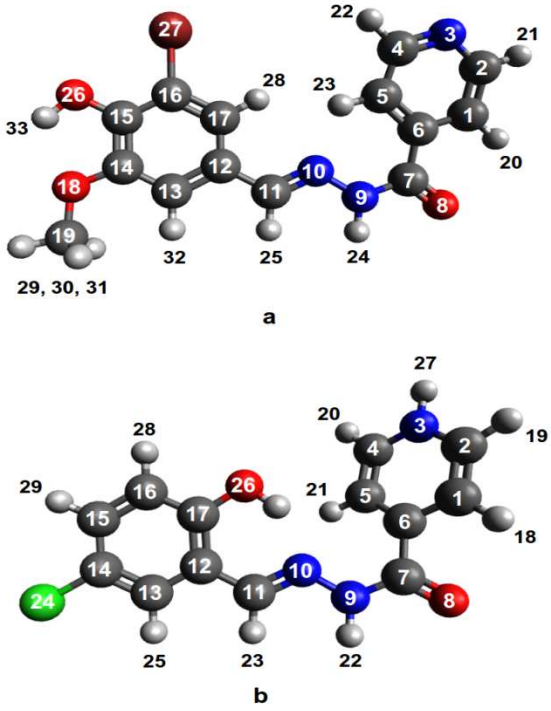

Figure S3. Numbering schemes used in the potential energy distribution analyses. **(a)** Scheme for INHVa (**1**) and INHBrVa (**2**). Position 27 is H and Br in (**1**) and (**2**), respectively. **(b)** Scheme for INHClSal (**3**) and INHBrSal (**4**). Position 24 is Cl and Br in (**3**) and (**4**) respectively.

Graphical Abstract

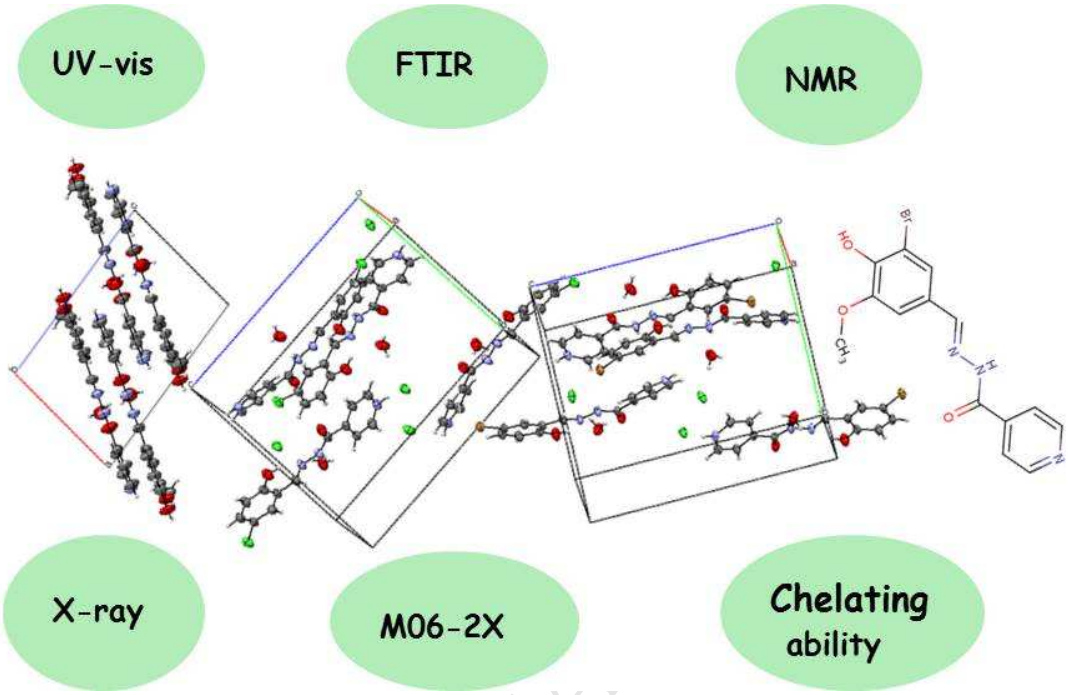

Highlights

- Hydrazones of hydroxylbenzaldehydes and antituberculous agent Isoniazid.
- Three crystal structures solved by X-ray diffraction methods.
- Spectroscopic (FTIR, electronic and NMR) analysis.
- Theoretical study based on DFT.